EFFECT OF BRIGHT SUNSHINE DURATION ON THE SELECTION OF SETTLEMENT LOCATION: A GIS METHOD APPLIED TO ÇANKIRI PROVINCE

A THESIS SUBMITTED TO
THE GRADUATE SCHOOL OF NATURAL AND APPLIED SCIENCES
OF
THE MIDDLE EAST TECHNICAL UNIVERSITY

BY

EMRE ERDOĞAN

IN PARTIAL FULFILLMENT OF THE REQUIREMENTS FOR
THE DEGREE OF MASTER OF SCIENCE

IN

GEODETIC AND GEOGRAPHIC INFORMATION TECHNOLOGIES

SEPTEMBER 2004

Approval of the Graduate School of Natural and Applied Sciences

_____

Prof. Dr. Canan ÖZGEN
Director

I certify that this thesis satisfies all the requirements as a thesis for the degree of Master of Science.

_____

Assoc. Prof. Dr. Oğuz IŞIK
Head of Department

This is to certify that we have read this thesis and that in our opinion it is fully adequate, in scope and quality, as a thesis for the degree of Master of Science.

_____

Prof. Dr. Vedat TOPRAK
Supervisor

Examining Committee Members

Assoc. Prof. Dr. Oğuz Işık	METU CP	_____
Prof. Dr. Vedat TOPRAK	METU GEOE	_____
Assist. Prof. Dr. Mustafa Türker	METU GGIT	_____
Assist. Prof. Dr. Zuhal Akyürek	METU GGIT	_____
Dr. Arda Arcasoy	SRK Consulting	_____

I hereby declare that all information in this document has been obtained and presented in accordance with academic rules and ethical conduct. I also declare that, as required by these rules and conduct, I have fully cited and referenced all material and results that are not original to this work.

Name, Last name :

Signature :

ABSTRACT

EFFECT OF BRIGHT SUNSHINE DURATION ON THE SELECTION OF SETTLEMENT LOCATION: A GIS METHOD APPLIED TO ÇANKIRI PROVINCE

Erdoğan, Emre
M. Sc., Department of Geodetic and Geographic Information Technologies
Supervisor: Prof. Dr. Vedat Toprak
September 2004, 84 pages

This study derives a method that seeks a possible relationship between settlement site locations and sunrise-sunset times of those locations using Geographical Information Systems. The method is applied to Çankırı province, which is located at northeast of Ankara and covers approximately an area of 8380 km^2.

Three main data sets of the study area are used in this thesis: 1) Settlement data containing the coordinates, IDs and names of the 891 settlement points, 2) Topographic data containing the coordinates and digital elevation values of all raster pixels 3) Bright sunshine duration data (BSD) composed of the difference between sunset and sunrise times for all raster pixels.

In the first step of this study, sunrise and sunset times of the study area are calculated with an algorithm that uses Digital Elevation Model. This algorithm is developed specifically for computing those times over a topographic surface which may delay the sunrise time or bring forward the sunset time, thus reducing the BSD. In the second step, unsuitable landforms for settlement are clipped out from the study area based on the thresholds derived from elevation, slope and aspect parameters. Then, BSD histograms and statistics of the settlements and

study area are compared for each of the 12 months and for the average of 12 months. Finally, neighborhood analysis on settlements is carried out by comparing the BSD values of each settlement with the BSD characteristics of circular buffer surrounding the settlement.

The main conclusion derived from above mentioned analysis is that the BSD does not directly affect the selection of the settlement sites.

Keywords: settlement location, sunrise, sunset, topography, Turkey

ÖZ

GÜNEŞLENME SÜRESİNİN YERLEŞİM YERİ SEÇİMİNDE ETKİSİ: ÇANKIRI İLİNE UYGULANAN BİR CBS YÖNTEMİ

Erdoğan, Emre
Yüksek Lisans, Jeodezi Ve Coğrafi Bilgi Teknolojileri
Tez Yöneticisi: Prof. Dr. Vedat Toprak
Eylül 2004, 84 sayfa

Bu çalışma, Coğrafi Bilgi Sistemleri (CBS) kullanarak yerleşim yeri ile gündoğumu-günbatımı zamanı arasındaki olası ilişkiyi araştıran bir yöntem geliştirmeyi amaçlamaktadır. Bu yöntem Ankara'nın kuzeydoğusunda yer alan ve yaklaşık 8380 km^2 alana sahip olan Çankırı iline uygulanmıştır.

Bu tezde çalışma alanına ait 3 ana veri kümesi kullanılmıştır: 1) 891 yerleşimin kimlik, ad ve koordinat değerlerini içeren yerleşim veritabanı, 2) Tüm piksellerin koordinatlarını ve sayısal yükselti değerlerini içeren topoğrafya veritabanı, 3) Tüm piksellerin günbatımı ile gündoğumu zamanlarının farkından oluşan güneşlenme zamanları veritabanı.

Bu çalışmanın ilk aşamasında sayısal yükselti modelini kullanan bir algoritmayla gündoğumu ve günbatımı zamanları hesaplanmıştır. Bu algoritma, anılan zamanları gündoğumu zamanını geciktiren veya günbatımı zamanını önceye alan ve böylelikle güneşlenme zamanını azaltan topoğrafik bir yüzey üzerinde hesaplamak amacıyla geliştirilmiştir. İkinci aşamada, yerleşime uygun olmayan alanlar yükseklik, eğim ve bakı parametrelerinden elde edilen eşik değerleri kullanılarak çalışma alanından çıkarılmıştır. Yerleşim yerlerinin ve çalışma alanının güneşlenme zamanı histogramları 12 ay ve 12 ayın ortalaması ile

karşılaştırılmıştır. Son yorumlara ulaşabilmek için, yerleşim yerlerinin ve yerleşim yerlerini çevreleyen dairesel tampon alanların güneşlenme zamanı karakteristikleri analiz edilerek komşuluk analizi gerçekleştirilmiştir.

Yukarıda bahsedilen analizler sonucu güneş alma zamanlarının yerleşim yeri seçimini doğrudan doğruya etkilemediği sonucuna ulaşılmıştır.

Anahtar kelimeler: yerleşim yeri, gündoğumu, günbatımı, topoğrafya, Türkiye

To
my father Fikret
and
my friend Hande

ACKNOWLEDGEMENTS

I would like to express my sincere thanks to the following people:

My advisor, **Prof. Dr. Vedat Toprak**, not only for sharing his precious information with me but also for supporting me by moral means.

Assist. Prof. Dr. M.Lütfi Süzen, **Dr. Arda Arcasoy** and **Assist. Prof. Dr. Nuretdin Kaymakçı,** for their valuable contributions, guidance and support.

My Professors in Geodetic and Geographic Information Technologies Department, METU, for sharing their precious instructions with me for 2 years.

Ali Özgün Ok, for being a good friend and supporter of mine.

My family, for their encouragement and moral support.

TABLE OF CONTENTS

LIST OF TABLES

TABLES

LIST OF FIGURES

FIGURES

ABBREVIATIONS

ANSI : American National Standards Institute
BSD : Bright Sunshine Duration
DEM : Digital Elevation Model
DTM : Digital Terrain Model
GIS : Geographical Information System
NASA : National Aeronautics and Space Administration
NGA : National Geospatial-Intelligence Agency
NOAA : National Oceanic and Atmospheric Administration
SRTM : Shuttle Radar Topography Mission

CHAPTER 1

INTRODUCTION

1.1 Purpose and Scope

In determining the suitable places for settlement areas, many factors should have been taken into consideration by past and current civilizations. Mankind has always been in search of settling down in the areas which can serve them a higher standard of living. Studies show that many natural resources, topographical and morphological features, and landform type had an influence in determining the original settlement places as will be explained in the following sections. Among these factors, sunrise and sunset times of the location have an important effect in agricultural and daily-life activities, and thus, may be one of the critical factors in choosing the settlement places.

The main objective of this study is to derive a methodology to find a possible relationship between the settlement location and sunrise-sunset times of that location. Sunrise-sunset time of a specific location is affected by the topographic features surrounding the location. An elevated topographic feature existing in the eastern horizon shifts the sunrise time ahead of the normal sunrise time, and similarly, an elevated topographic feature existing in the western horizon shifts the sunset time before the normal sunset time. Therefore, the actual sunrise-set times may differ considerably from normal (astronomical) sunrise-set times. In this study, a new use of DTM is described in the calculation of visual sunrise and sunset times, thus, topography is assumed to be the major factor controlling the relationship between the sun times and the settlement.

In this study, only the effect of the sunrise-sunset times will be investigated in order to reveal the effect of BSD on settlement selection. Any other factor, such as the rock type, proximity to natural resources, is not taken into consideration.

Three main data sets are used in this study:

- Sun time data (BSD data): These data can be divided into two categories:
  - Unobstructed times: Sunrise and sunset times for all pixels in the study area and for 891 settlement points, which does not take the effect of topography into consideration. This data set assumes that there are no topographical obstructions present on the earth surface. Since the elevation is constant, sunrise-sunset times are almost same throughout the study area.
  - Topographic (obstructed) times: Sunrise and sunset times for all pixels in the study area and for 891 settlement points, which is calculated by a tailored algorithm and takes the effect of topographic features into consideration. Since the elevation varies, sunrise-sunset times differ throughout the study area.

  The difference between sunset and sunrise times gives the total visible sun time throughout the day, which is hereafter referred to as "BSD" in this thesis.
- Settlement data: Contains the coordinates, Id's and names of the settlement points in the study area.
- Topographic data: Contains the coordinates and digital elevation values of all points in the study area.

1.2 Study Area

The methodology in this thesis is applied to Çankırı province, which is located northeast of Ankara and covers approximately an area of 8380 km^2 (Figure 1.1). Çankırı province is selected because the terrain is mountainous and rough, which intensely vary in elevation values. These features emphasize the effect of topographic features relative to sunrise and sunset times.

The projection system of the area is Universal Transverse Mercator (UTM) with 36 North Zone in European 1950-Mean datum and International 1909/1924 / Hayford 1910 ellipsoid.

The major streams in the area are Kızılırmak, Gerede, Devrez and their tributaries. Northern part of the area is represented by mountains and valleys oriented mainly in NEE-SWW direction as illustrated by the course of Gerede and Devrez rivers in Figure 1.1. This is due to the presence of the active fault zone (North Anatolian Fault zone) that crosses the province along its northern part.

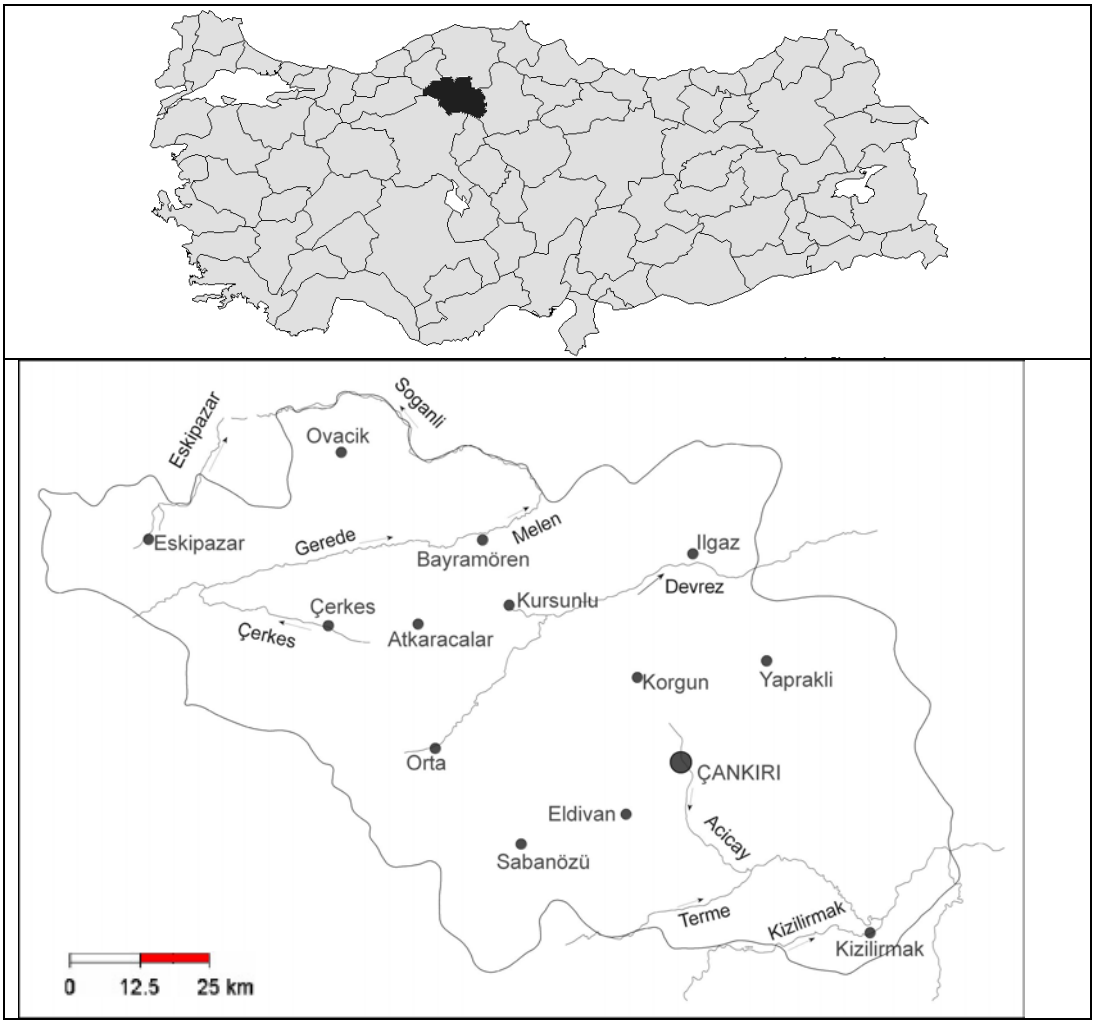

Figure 1.1: Location map of the study area. Outer solid black line is Çankırı province boundary. Points indicate major settlements. Lines show major streams.

1.3 Method of Study

This thesis is completed as an office work consisting of calculating sunrise-set times over the mountainous horizon and analyzing / interpreting the calculation results using the following software packages:

Table 1.1: Software packages used during this study

Software	**Purpose:**
Borland ANSI C Editor & Compiler	Programming sunrise-set calculation
TNT Mips 6.8	GIS applications
Microsoft Excel 2000	Generating histograms and charts
Golden Software Surfer 8	Generating contour maps and grid maps
SPSS 11.5	Statistical calculations
Rockware Rockworks 2002	Generating histograms and charts

1.4 Organization of Thesis

The rest of this thesis is organized as follows:

- Chapter 2 contains the literature survey and reviews of necessary information on solar and astronomical concepts, and sun position determination.
- Chapter 3 presents data that are used in the study and the algorithm for obtaining BSD data set.
- Chapter 4 describes the method and the analysis carried out for the investigation of the relationship between settlement locations and the BSD.
- Chapter 5 contains the discussions, conclusions and recommendations that have been revealed as an outcome of this study.
- Three Appendices are given at the end of the main body as: A) General Solar Position Calculations, B) Algorithm for sunrise/sunset and BSD calculations, and C) Settlement data

1.5 Previous Works

Past studies related with the subject of this thesis can be grouped into two categories:

1. Studies seeking a possible relationship between the settlement locations and an attribute of the settlement locations, i.e. investigation of a relationship between settlement sites and landform.
2. Studies focusing on the computation of solar parameters on Earth surface, such as the calculation of solar radiation or calculation of sunrise-sunset times.

1.5.1 Studies on Settlement Site – Attribute Relationship

There are a large number of references that seek a relationship between the site of settlement and the natural environment that plays a role in the selection of this site. These studies can be grouped into three categories as 1) Investigation of various natural parameters in the site selection of the settlement such as landform, vegetation, main transportation routes etc., 2) Investigation of the site selection with respect to a single feature existing in the vicinity of site such as hot springs, presence of a specific stone or mine (obsidian, marble) etc., 3) GIS applications in the evaluation of the parameters in the site selection.

Among these studies, however, there is not any work that aims to investigate the relationship between the site of the settlement and the sunrise-sunset times. In this respect, this thesis forms the first example of its topic. Other related works similar to the subject of this thesis are briefly explained below in chronological order.

Noss (1985) investigated the location and movement of settlements in interior Alaska from an ecological perspective. He did a path analysis and demonstrated that population density has been primarily determined by regional salmon abundance from 1880 to the present. This exposed that trend surfaces of salmon abundance are virtually identical to relative population density.

Hunt (1990) studied the critical elements that affect the location of 224 archaeological village sites of Western New York between years 1000-1650 AD. These elements include climate, physiography, subsistence strategy, social organization, and settlement patterns. The site data, climatic data, and soil data are linked to several digitally constructed maps. As a result of this study, climate is found to be the major factor for moving the settlements. Village sites are moved away from areas of high snowfall and areas associated with a shorter growing season. Moreover, villages are located in areas that have highly productive soils.

Stea and Turan (1993) in their voluminous and detailed work studied the effect of natural environment on “placemaking” in two regions (central Anatolia and Pajarito Plateau of New Mexico). In comparing settlement systems in two geologically and morphologically similar but culturally different places, they address how and why people build and live the way they do. According to them, the “placemaking” is simultaneously economic, cultural, political and an integral part of one or more modes of production.

Lourens (1994) tried to identify areas that are suitable for urban settlement in South Africa. This region is densely populated and divided into tribal areas, which yielded to unplanned and uncontrolled settlement. At the first stage of this study, the factors that have an influence in settlement are identified. These factors are found to be hydrology, geology, soil types, topography, and nature conservation. A probability index is given to each of the factors and a general probability model is built up. Later, current settlements are compared with this model. Results show that settlement take place in areas that are not suitable for building and settlement and huge areas with high agricultural potential have been invaded. This study reveals that soil surveys and future planning have to be done for future settlements.

Kuiper and Wescott (1999) emphasized the use of GIS based predictive mapping to locate areas of high potential for prehistoric archaeological sites. They used the knowledge of the environmental variables influencing activities of original inhabitants to produce GIS layers representing the spatial distribution of these

variables. Distance to water, type of water source, soil type, elevation, slope-aspect and topographic settings are created and then analyzed to identify locations where combinations of environmental variables match the patterns observed at known prehistoric sites. By this means, they tried to locate high potential areas for prehistoric sites in a largely unsurveyed area.

Bradford (2001) did an archaeological study in Windward Island of France by constructing settlement patterns according to environmental factors and investigated the correlation of the sites within environmental factors and landform adaptation. She produced a regional archaeological site database and identified several environmental factors, which may have influenced the locational decision-making process of prehistoric people. She identified the main environmental factors to be: (1) Location within one-half mile of the present coast, (2) Location below fifty feet elevation, (3) Location near reefs, and (4) Associated with one of five types of vegetation. This study contributes to the understanding of social and demographic changes of ancient settlements in respect to environmental parameters.

Özdemir (2002) studied on deriving a methodology to find a possible relationship between the original settlement and rock types existing in Çankırı province, using GIS. Main assumption of this study is that, people take the rock type into consideration when they select a site to settle. During this selection, topography is assumed to be the major factor controlling the relationship between the rock type and the settlement. Any other external factor is not taken into consideration in the evaluation of such a relationship. She used three main data sets, namely, rock types, settlements and topography. The methodology is based on the elimination of the rock types that are not suitable due to topographic conditions and then evaluation of the percentages of settlements in the remaining rock types.

Maizel (2003) presented the historical interrelationships between farmland and population settlement patterns. She examined simple overlays of counties with historical population and farmland data, together with national soils and topographic data layers. She focused on the farmland usage under urban

influence and concluded that a significant portion of the United States' prime farmlands has been lost to metropolitan development in the past 100 years by rationing the urban usage layer and farmland usage layer.

Sürmeli (2003) investigated the relationship between landform classes and settlement sites in Çankırı province using GIS. Her study does not take the factors influencing the settlement locations other than topographic landform conditions into consideration. The method is composed of three major steps. In the first step, topographically unsuitable areas are removed. In the second step, relationship between the settlements and landform is analyzed. In the last step, further analysis of the relative location of settlements within the landform is carried out for the final investigation of this relationship.

1.5.2 Studies on Solar Parameters

Kumar *et al*. (1997) developed one of the first GIS based solar radiation models. The model presented here uses a DEM to compute potential direct solar radiation over a large area. The model may be modified to include diffuse radiation (the scattered radiation that reaches the ground), as well as parameters such as cloud cover and water content of the atmosphere. They stated that the solar radiation received at a site is dependent on:

- Position of sun in the sky
- Solar azimuth angle
- Solar altitude angle
- Solar declination angle
- Solar flux outside the atmosphere
- Optical air mass (air mass ratio)
- Water vapor and aerosol content of atmosphere
- Slope
- Aspect
- Shading
- Elevation of site

Variables such as solar altitude and solar azimuth angles change continuously throughout the day so they have to be calculated every time the intensity of solar radiation is computed. Another important factor which needs to be calculated is shading by topographic features. Aspect and slope may be easily calculated from a DEM.

Keller and Hall (1999) described a new use of DTM in the calculation of highly accurate visual sunrise and sunset times. They employed ray tracing to determine the effect of atmospheric refraction through a simplified layered atmosphere. A general expression for the atmospheric refraction was determined from these calculations as a function of the observer's height for two model atmospheres knows as the summer and winter atmospheres. These expressions determine the magnitude of the refraction as a function of apparent view angle of the observer. They also determined a simplified expression for the effect of atmospheric refraction on the vertical angular profile of the mountainous horizon as calculated from the DEM. These expressions are then used in calculating the apparent position of sun as a function of time.

Hofierka and Suri (2002) stated that solar radiation incident on the Earth's surface is a result of complex interactions of energy between the atmosphere and surface. At global scale, the gradients of radiation are caused by the geometry of the earth and its rotation and revolution about sun. At regional and local scales, terrain (relief) is the major factor modifying the distribution of radiation. Variability in elevation, slope and aspect and shadows cast by terrain features creates strong local gradients. The radiation, selectively attenuated by the atmosphere, which is not reflected or scattered and reaches the surface directly is beam (direct) radiation. The scattered radiation that reaches the ground is diffuse radiation. The small part of radiation that is reflected from the ground onto the inclined receiver is reflected radiation. These three components of radiation together create global radiation. A new GIS-based solar radiation model modeling the global radiation is developed in scope of this study using the open source environment of GRASS GIS platform.

CHAPTER 2

FUNDAMENTALS OF SUN POSITION CALCULATION

The visible sunrise and sunset times are defined as those times at which the sun rises and sets, respectively, over the horizon. The earth's revolution about the sun and about its own north-south axis causes the angle of the sun (its altitude above the horizon and direction) to change continuously. These changes take place in regular and thus in predictable patterns. These patterns can be used to determine when the sun will rise and set on any day and for any place, how high the sun will be in the sky at a particular hour. Some of the calculations for these items can be quite laborious and complex and should be left to computer applications.

In this chapter, key concepts of solar positioning and sun's daily path across the sky are described in order to build a fundamental background for the rest of this thesis. Afterwards, the method used to calculate the sunrise and sunset times is introduced assuming that the western and eastern horizons are unobstructed by topographical features such as mountains.

2.1 Key Concepts of Solar Positioning

2.1.1 Solar Altitude

Sun's altitude (Solar altitude) is the angle formed by imaginary lines drawn from the sun to an observer, and from the observer to the horizon (Figure 2.1) (Nelson, 2000). Positive numbers of θ indicate values above the horizon, and negative numbers indicate below the horizon. Negative numbers are usually used in terms of how far below the horizon the sun is located at a given time.

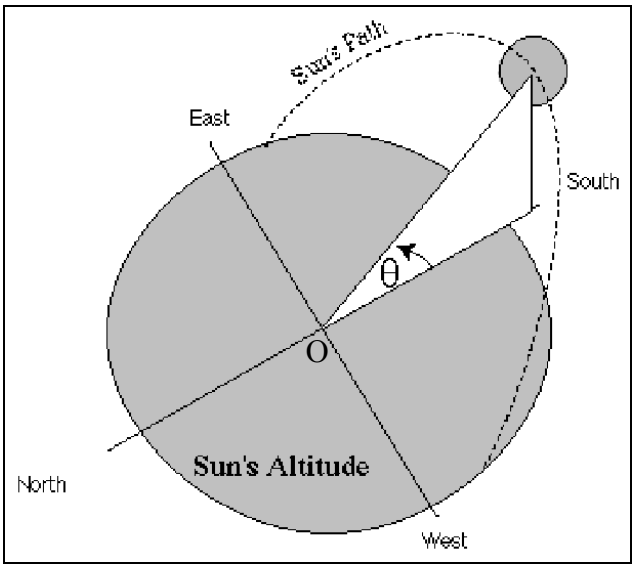

Figure 2.1: Solar Altitude Angle (θ) observed from point O.

2.1.2 Solar Zenith Angle

Solar zenith angle is the angle between the observer's zenith point (directly the overhead) to the sun's position in the sky (NASA, 1999) (Figure 2.2). The zenith angle and the sun's altitude are complementary angles.

Solar zenith angle + Solar altitude angle = 90°

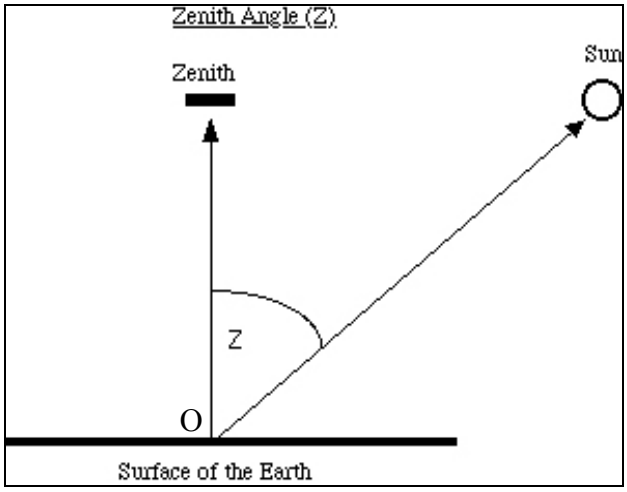

Figure 2.2: Solar Zenith Angle (Z) observed from point O.

2.1.3 Solar Azimuth

Solar azimuth is the angle of the direction that the sun appears to be over with 0° being north, 90° being east, 180° being south and 270° being west measured in clockwise direction (NOAA glossary, 2004) (Figure 2.3). Figure 2.4 illustrates the altitude, zenith and azimuth angles in one figure.

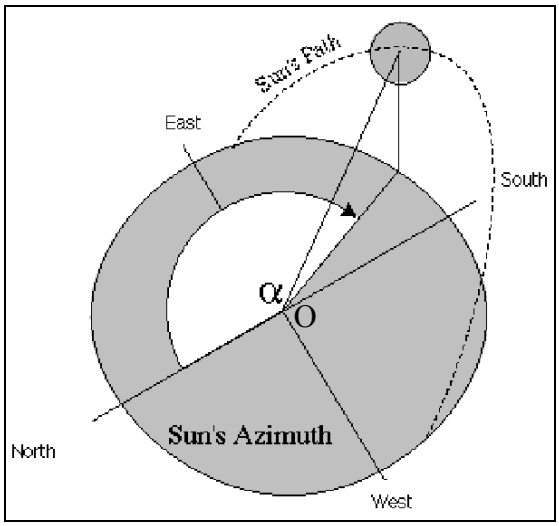

Figure 2.3: Solar Azimuth Angle (α) observed from point O.

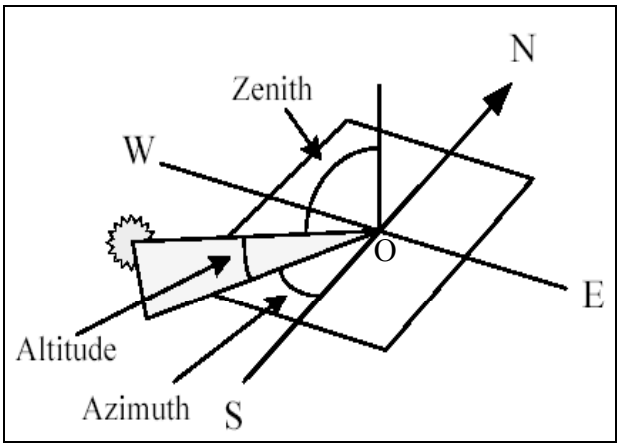

Figure 2.4: Altitude angle, Zenith angle, Azimuth angle observed from point O.

2.1.4 Solar Declination Angle

Solar declination is the angle between a plane perpendicular to incoming solar radiation and the rotational axis of the earth (NASA, 1999). The earth's axis is tilted about 23.5°. The solar declination angle varies from +23.5° on June 21/22 when the earths' axis is tilted toward the sun, to -23.5° on December 21/22 when the earths' axis is tilted away from the sun (Figure 2.5). The solar declination angle is 0° on equinox dates. Changes in the solar declination angle as the earth revolves around the sun create cyclic changes in solar radiation. These radiation changes contribute to cyclic weather changes that are called seasons.

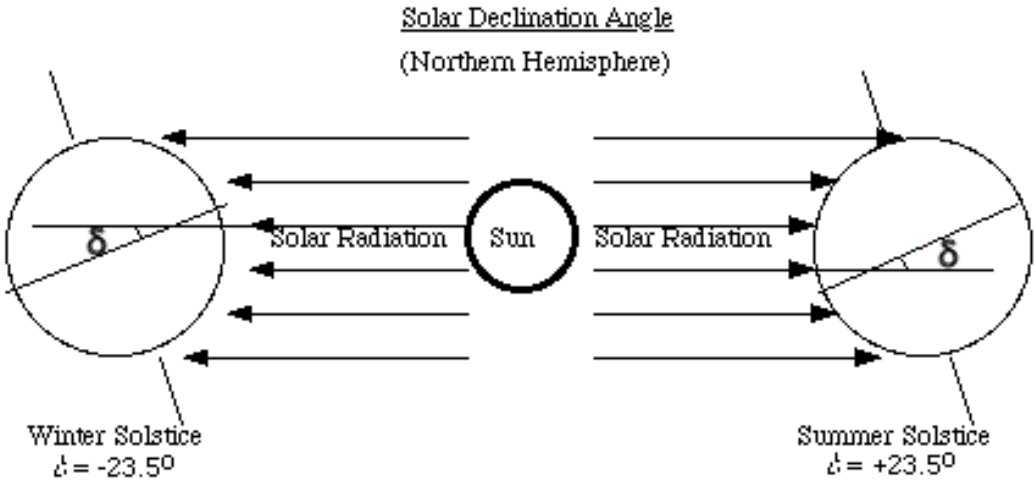

Figure 2.5: Solar Declination Angle (δ) shown for summer solstice and winter solstice dates.

2.1.5 Sun's Daily Path Across the Sky

At any time of the year and day, the sn's position with reference to the horizon can be expressed through a combination of two values, the altitude and the azimuth. In Figure 2.6, sun's position can be expressed by azimuth (α) and altitude (h) angles. The dashed line shows the daily path of the sun from an observer's view with reference to the horizon.

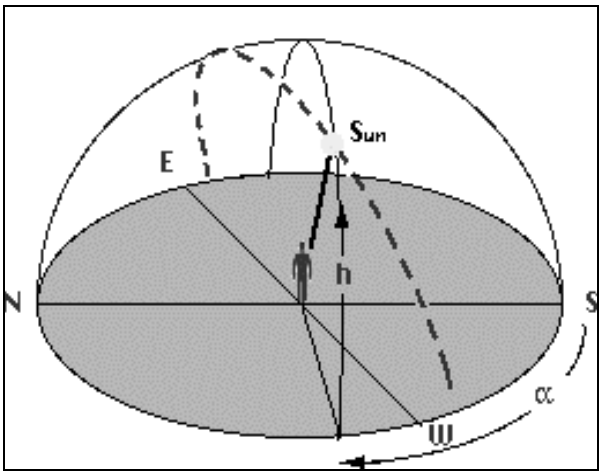

Figure 2.6: Dashed line shows the Sun's daily path across the sky from an observer's view. α is the azimuth angle, h is the altitude angle.

For a fixed point on earth surface, sun follows a different path across the sky for each day of the year. As solar declination varies within a year, sunrise-sunset points and the path of the sun across the sky change. Figure 2.7 shows the path of the sun for 4 different sample dates in a year for a point located in Northern Hemisphere.

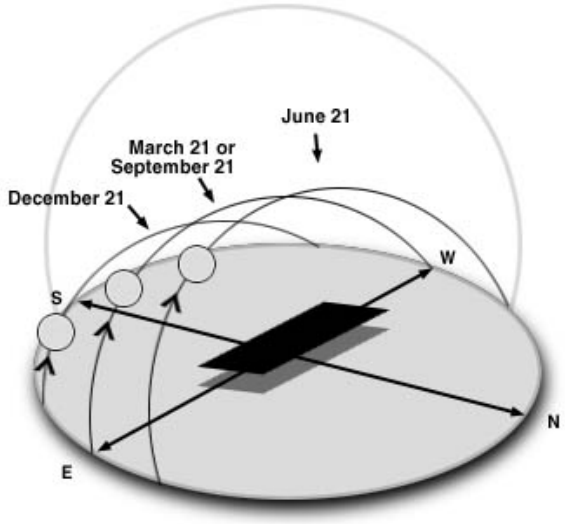

Figure 2.7: Daily path of the sun shown for 4 different dates. Three circles represent the Sun.

The relationship between azimuth and altitude can be graphically represented through the sun-path diagrams for a site. One of these methods is “Cylindrical Sun Path Diagram” method developed by Mazria (1979) (Figure 2.8). This chart is a vertical projection of the sun's path as seen from the earth. It could be said that this chart is an earth base view of the sun's movement across the skydome.

In the Cylindrical Sun Path Diagram, the bearing is marked at the base (horizontal axis), and the altitudes on the vertical axis. Each curve shows the daily movement of the sun for the mentioned dates written above the curve. The location of the sun can be determined by using the horizontal and vertical axises (intersection of the altitudes and the azimuths) (Mazria, 1979) (Figure 2.9).

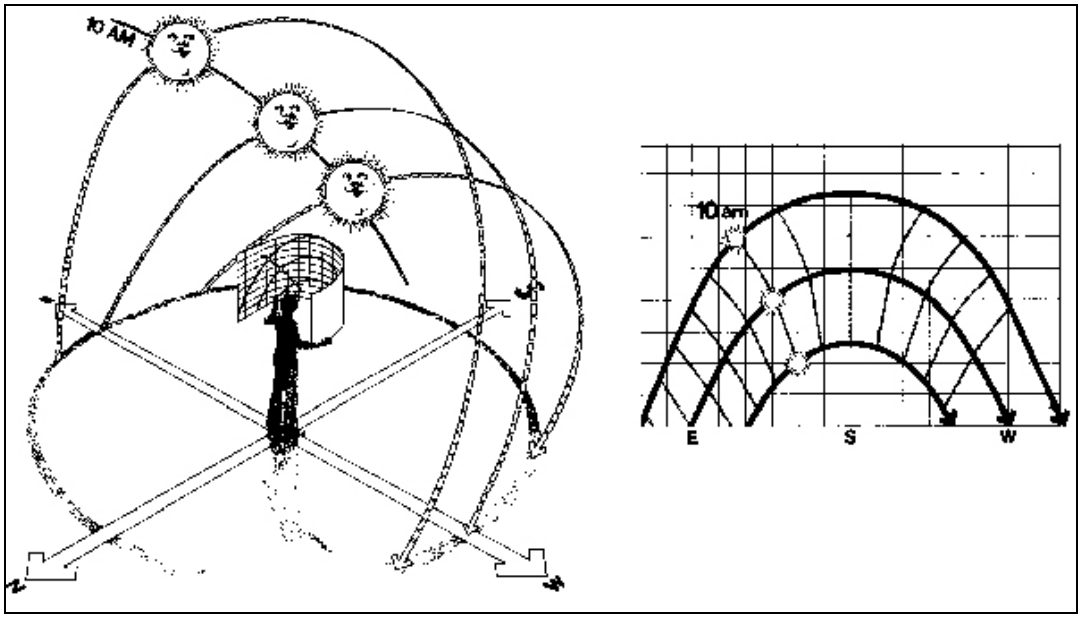

Figure 2.8: Plotting of a cylindrical Sun Path Diagram (after Mazria, 1979).

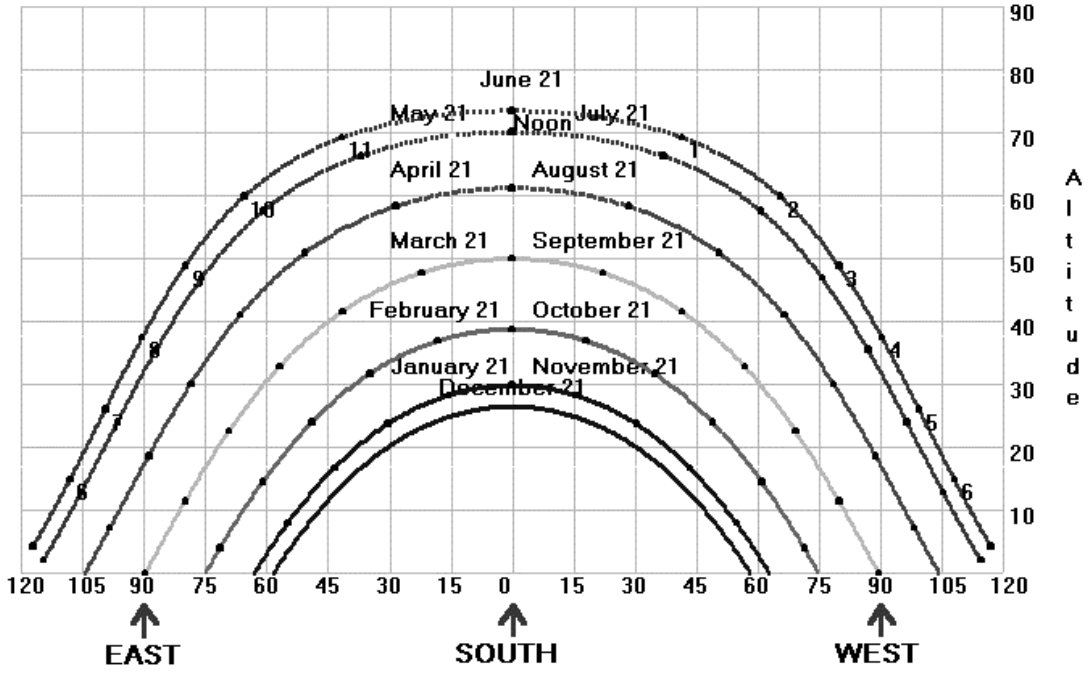

Figure 2.9: Cylindrical Sun Path diagram for 40° North (after Mazria, 1979).

From Figure 2.9, it can be deduced that:

- On March 21 and September 21 the sun rises approximately 90° east of south and sets approximately 90° west of south,
- On December 21 the sun rises approximately 60° east of south and sets approximately 60° west of south. Minimum altitude value (~25°) is observed throughout the year.
- On June 21 the sun rises approximately 120° east of south and sets approximately 120° west of south. Maximum altitude value (~75°) is observed throughout the year.

In the northern hemisphere, in the winter time, the sun rises and sets at azimuth angles that are closer to south, and receiving sun's radiated energy at lower altitudes causes the incident energy on the earth to be less compared to summer. In the summer time, the sun rises and sets at azimuth angles that are closer to north, and receiving sun's radiated energy at higher altitudes causes the incident energy on the earth to be more compared to winter.

2.2 Sunrise-Sunset Calculation Formulae

Throughout this thesis, general solar calculation formulae obtained from NOAA are taken as reference formulas and form a basis for the sunrise-sunset calculation algorithm. These formulations are given in Appendix A.

CHAPTER 3

DATA USED IN THE STUDY

This chapter describes the sources, properties and characteristics of the data used in the study. Three data sets are used in this study. These are:

1) Topographic data
2) Settlement data
3) BSD data

Topographic and settlement data already exist before starting this thesis. BSD database is produced by a specifically developed algorithm tailored at calculating the sunrise and sunset times using the existing topographic and settlement data. The algorithm is also introduced in this chapter.

3.1 Topographic Data

Topographic data is the DEM at 90 m pixel resolution and 16 m vertical accuracy obtained from SRTM. SRTM is an international project pioneered by NGA and NASA. SRTM obtained elevation data on a near-global scale to generate the most complete high-resolution digital topographic database of the earth. SRTM consisted of a specially modified radar system that flew onboard the Space Shuttle Endeavor during an 11-day mission in February of 2000 (NASA SRTM, 2004)

The study area is extracted from the original SRTM DEM of the whole Turkey at using TNT Mips software. The extracted area is re-sampled in order to make it 100 m cell size for both column and line. The resultant area contains 1540 columns and 959 lines, summing up to 1476860 cells. Elevation, slope and aspect maps are derived using TNT Mips software over the extracted study area.

3.1.1 Elevation Map

Elevation of the study area varies between 364 and 2398 meters and populates densely in the range of 550-1750 meters (Figures 3.1 and 3.2). The lowest elevations are dominant around the southeastern part of the area (particularly around the flood plains of the Kızılırmak River as shown in Figure 1.1), thus leading to a smoother surface. The highest elevations, on the other hand, can be observed around Ilgaz Mountains. The northern part of the area corresponds to the North-Anatolian fault zone, where the surface is comparably rough.

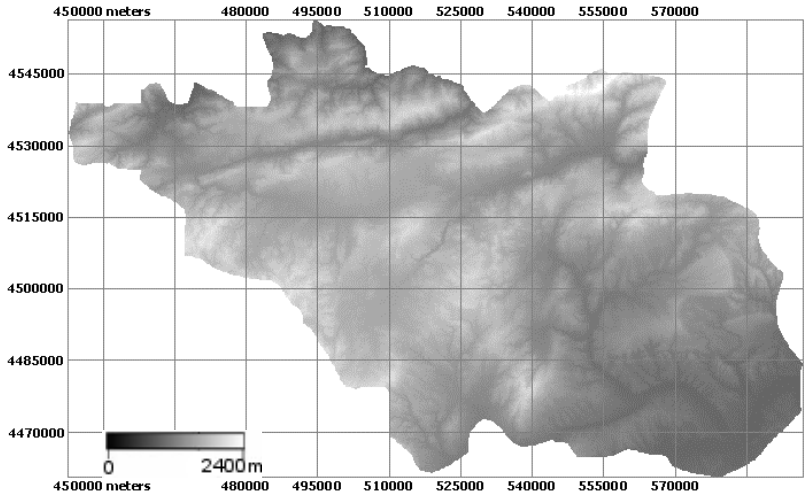

Figure 3.1: DEM of the study area.

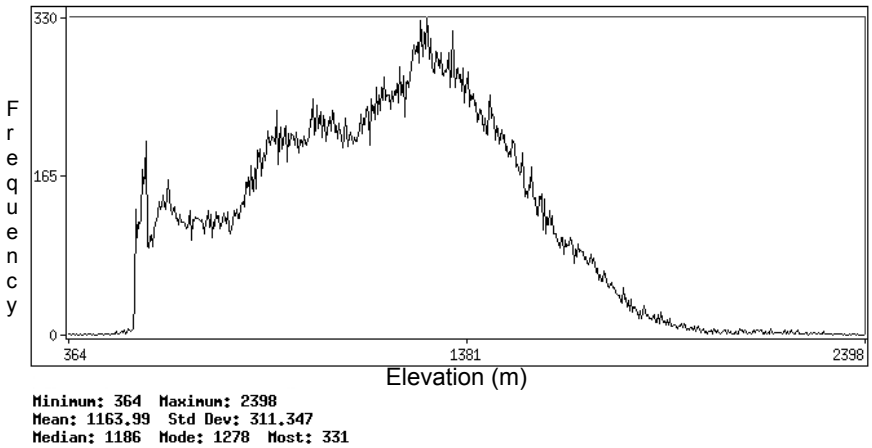

Figure 3.2: DEM histogram and statistics.

3.1.2 Slope Map

Slope map of the area is created from the DEM map shown in Figure 3.1. Slope of the study area varies between 0 and 48 degrees and populates densely in the range of 2-20 degrees (Figures 3.3 and 3.4). The slope map shows that northern part of the study area has higher slope values, whereas southeastern part of the area has lower slope values.

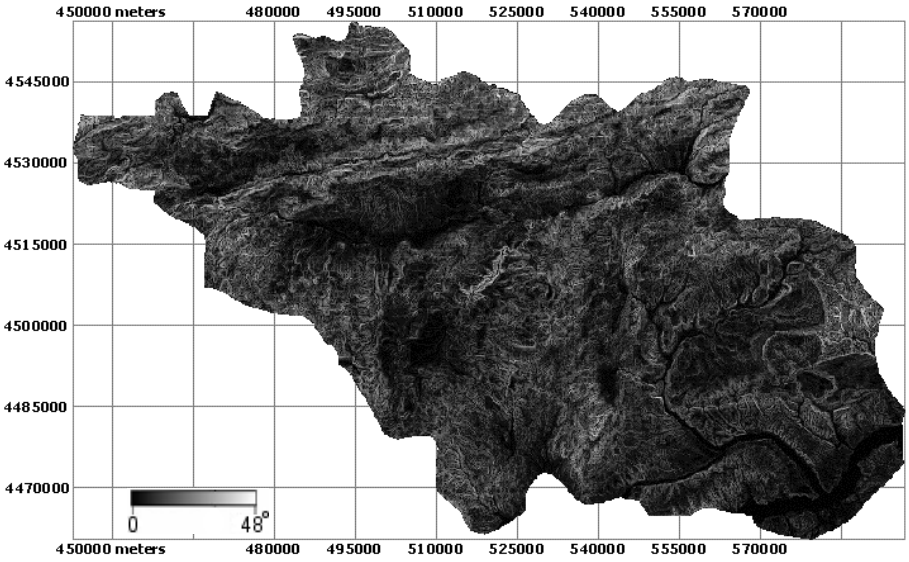

Figure 3.3: Slope map of the study area.

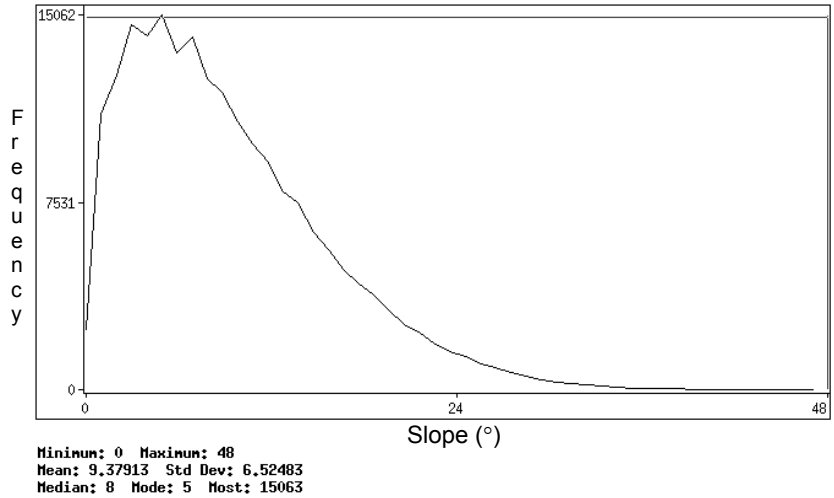

Figure 3.4: Slope map histogram and statistics.

3.1.3 Aspect Map

Aspect map of the area is created from the DEM map. Aspect of the study area varies between –1 to 360 degrees. Aspect values are grouped into 9 categories each representing a direction, in order to obtain more meaningful presentation, namely N, NE, E, SE, S, SW, W and NW. Table 3.1 shows the values and corresponding aspect ranges. Aspect map and its histogram are illustrated in Figures 3.5 and 3.6.

Table 3.1: Aspect ranges used in this study.

Degree	Class
-1	Flat
338-23	N
24-68	NE
69-113	E
114-158	SE
159-203	S
204-248	SW
249-293	W
294-337	NW

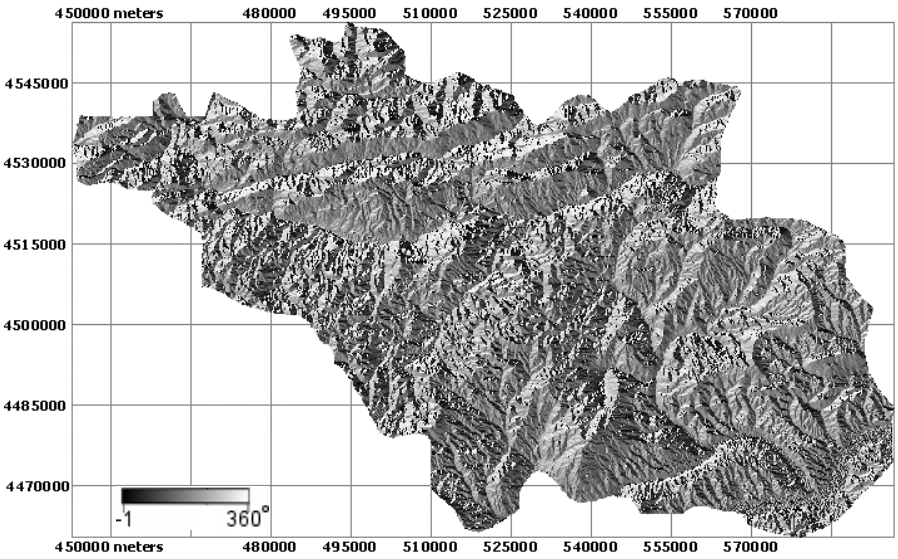

Figure 3.5: Aspect map of the study area.

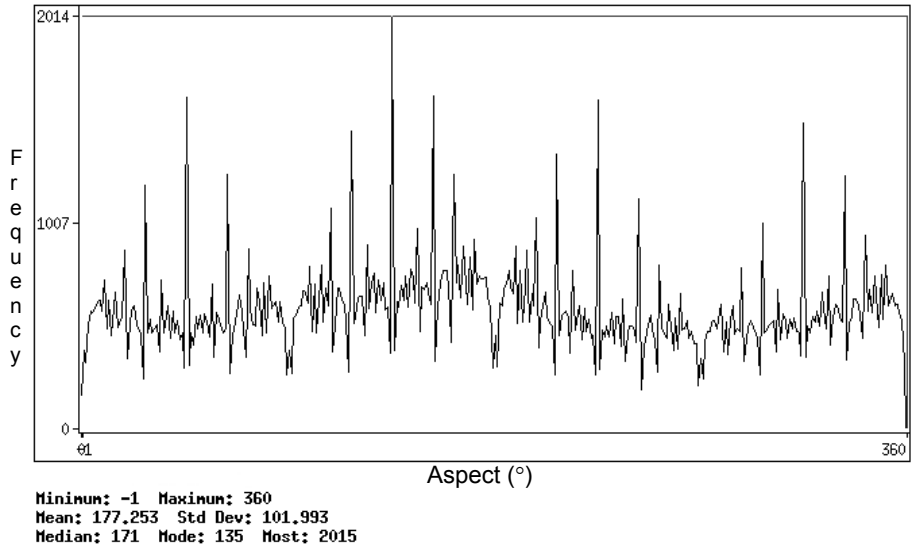

Figure 3.6: Aspect map histogram and statistics.

3.2 Settlement Data

Settlement data used in this study are obtained from Sürmeli (2003). She identified settlements using topographic maps of 1984-1997 at 1:25.000 scales. Identified settlements are then checked with settlement names listed in the map prepared by the Çankırı Municipality and found to be accurate. During the creation of the settlement database, following criteria are applied (Sürmeli, 2003):

- No distinction is made between the settlements considering their size, population or administrative classification. They are all counted in the database and considered as a single settlement.
- Each settlement is considered to be represented by a definite point on the map which is, most probably, the initial location of the settlement. Therefore, the later growth in size and boundaries of the settlement is not important in this study.

Under these assumptions, resultant settlement data contains 891 villages (Figure 3.7), each represented as a point object in a vector map and each showing the initial settlement place of the settlement, a settlement being a village, a district or a city.

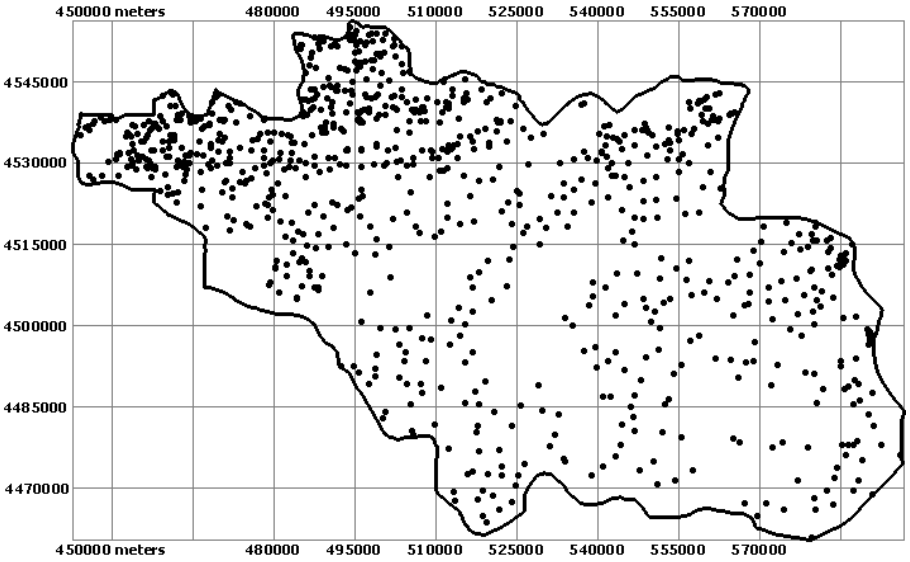

Figure 3.7: Location map of 891 settlements used in this study.

During this study, two different file formats of settlement data are used. First one is the point vector map of the settlements, which is introduced above. Second one is the ASCII text format, which can be converted into spatial database. This ASCII dataset details the properties of the settlements (Table 3.2):

- Id no
- Name of the settlement
- Topographic sheet number (at 1/25000 scale)
- Coordinates (2 columns: Easting and Northing)
- Topographic properties (elevation, slope , aspect)

Table 3.2: Sample settlement database in ASCII format

Id	Name	Topo-Sheet	Easting	Northing	Elev.	Slope	Aspect
1	Doganlar	F29-c3	494306	4543511	892	4	165
2	Sakarca	H32-a1	588203	4471546	551	2	316
3	Cukurkoy	F29-c1	488499	4552879	650	2	271
4	Guneykisla	H32-a4	590714	4469057	615	6	278
.	.	.	.	.	.	.	.
.	.	.	.	.	.	.	.

3.3 Daily Sunrise-Sunset and BSD Data

Prior to starting the thesis, no data was present covering the sunrise-sunset times over the study area. To make further analysis regarding the BSD of the pixels in the study area, a new algorithm is developed and programmed in ANSI C. This section describes this algorithm and the logic used to calculate solar times.

3.3.1 Calculation of BSDs

The visible sunrise and sunset times are defined as those times at which the sun rises and sets, respectively, over the mountainous horizon (Keller and Hall, 1999). These times change daily as the sun rises and sets over different terrain as it progresses in its apparent daily motion. The calculation of the visible sunrise and sunset times is therefore impossible without a topographical model of the eastern and western horizons, respectively.

The algorithm proposed to compute sunrise (or sunset) times at a fixed point over the mountainous horizon inspects for the eastern and southern horizons whether an obstacle is present which can hinder the sun and prevent it from being visible, thus delaying the sunrise time and bringing forward the sunset time. This approach helps to determine how to choose the DEM data for use in such computations. The extents and format of the input DEM data is determined as follows:

- A rectangular area is extracted in order to express the area in 2-dimensional matrix format, namely X and Y dimensions. This matrix format in turn can be expressed again as a 2-dimensional array structure in ANSI C. By this way, the elements of the array can be easily and quickly accessed. Each element of the array represents a pixel and contains the elevation value of that pixel.
- Approximately 20 km additional DEM data in East-West direction beyond Çankırı province boundary are included in the rectangular extraction. This makes the solar calculations possible for the settlement points that are located in the vicinity of the province boundaries. If some amount of margins from east and west is not included, solar computations for near-

boundary settlements would not produce accurate results since it would not be possible to inspect eastern and western horizons.

- Approximately 10 km additional DEM data in East-West direction beyond Çankırı province boundary are included in the rectangular extraction. This is because the sun does not always rise from true east and set at true west. Thus, it is needed to include some amount of margin from north and west in order to inspect sun at the time of rise or set.

Figure 3.8 shows the extracted DEM map for BSD calculations. It contains 1993 columns and 1176 lines, each cell having 100 m width and length.

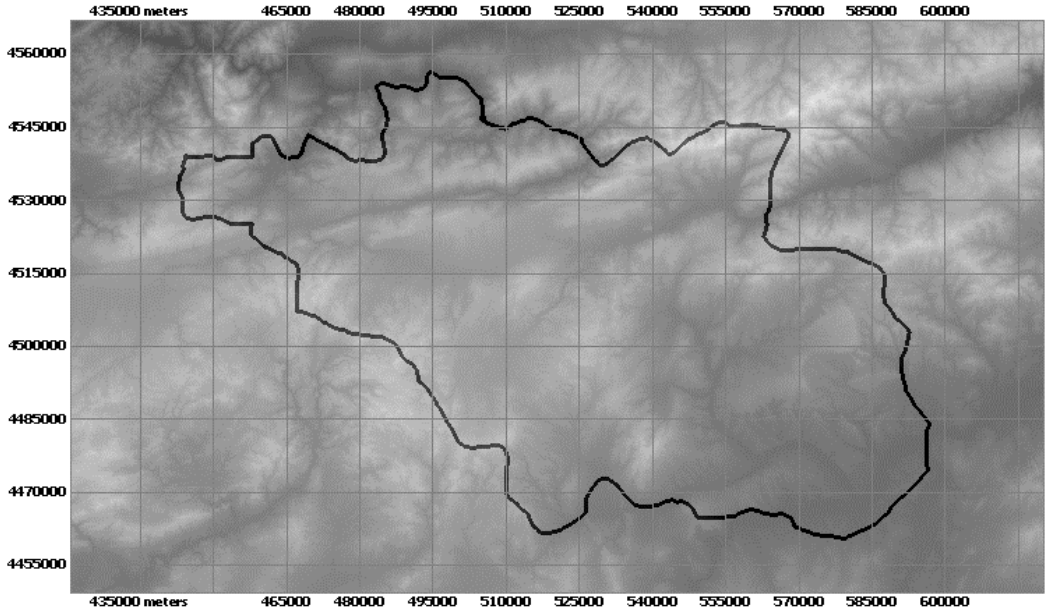

Figure 3.8: Rectangular area used in rise-set calculations.

Figure 3.8 is the visual representation of the extracted DEM in TNT Mips software RVC format, which is a special format of Microimages. Therefore, it is not suitable to be accessed and processed by an external program such as ANSI C programming language. To overcome this problem, the study area is converted to ASCII TXT format using the TNT Mips software “Export” utility. A sample from the

resultant converted file is shown Figure 3.9. Each number in the figure corresponds to the elevation value of a single pixel in the DEM. The original file contains elevation values of 1993 columns times 1176 lines, making a total of 2343768 numbers. The size of the file is approximately 13 MB.

```
+447 +455 +450 +452 +467 +492 +507 +485 +413 +379 +361 +357 +341 +326 +288
+265 +260 +277 +354 +354 +407 +399 +387 +386 +430 +448 +455 +455 +468 +482
+604 +520 +552 +561 +564 +578 +624 +661 +632 +610 +620 +656 +705 +730 +700
+554 +542 +552 +571 +564 +575 +604 +611 +612 +617 +625 +635 +640 +597 +590  .
.    .    .    .    .    .    .    .    .    .    .
.    .    .    .    .    .    .    .    .    .    .
```

Figure 3.9: Sample ASCII DEM input file showing the elevation values of raster pixels.

3.3.2 Algorithm for BSD Calculations

General solar position calculations used in this algorithm are based on NOAA document titled “General Solar Position Calculations”, given in Appendix A. This document gives necessary formulae for solar azimuth, altitude (zenith angle), and hour angle calculations. Additionally, basic sunrise-sunset calculation that assumes the eastern and western horizons are not obstructed by a topographic object (i.e. “flat”) is available in this document.

The algorithm explained in this section is developed specifically for computing sunrise and sunset times over a topographic surface. The wording “topographic surface” means a rough surface that has obstructions, which may delay the sunrise time or bring forward the sunset time, thus reducing the total visible sun time. This algorithm does not consider:

- The effect of atmospheric refraction caused by the nature of atmosphere
- The effect of cloud cover present on the atmosphere

The steps listed below are applied for a single pixel's rise-set calculation. The whole program is executed for each pixel in the extracted DEM for the sunrise calculation; the simplified algorithm is as follows:

Step 1: Calculate the normal (unobstructed) sunrise time, T

Step 2: Increase T by 1 minute, T = T + 1

Step 3: Calculate the current position of the sun at new T

Calculate the sun azimuth, AZI

Calculate the sun altitude, ALT

Step 4: Starting from the origin pixel, access each pixel that lies on the same direction with the AZI and find the obstruction that causes maximum obstruction angle, record the angle, MAXOBS.

Step 5: If

MAXOBS > ALT, sun is obstructed, does not rise yet.
Continue loop (go to Step 2).

Else,

Sun is not obstructed. Sun rises at this time.
Stop loop (go to Step 6).

Step 6: Record the final time as the sunrise time.

For the sunset calculation, a very similar algorithm is used:

Step 1: Calculate the normal (unobstructed) sunset time, T

Step 2: Decrease T by 1 minute, T = T - 1

Step 3: Calculate the current position of the sun at new T

Calculate the sun azimuth, AZI

Calculate the sun altitude, ALT

Step 4: Starting from the origin pixel, access each pixel that lies on the same direction with the AZI and find the obstruction that causes maximum obstruction angle, record the angle, MAXOBS.

Step 5: If

MAXOBS > ALT, sun is obstructed, already in set state.
Continue loop (go to Step 2).

Else,

Sun is not obstructed. This is the last time Sun is visible from the origin pixel. Sun sets at this time.

Stop loop (go to Step 6).

Step 6: Record the final time as the sunset time.

For the sunrise, the algorithm starts calculation with the normal (unobstructed) sunrise time, and iterates by increasing this time by one minute, as it is assumed that the unobstructed rise time is delayed due to an obstruction located on the sunrise direction. Step 4 is the most complex and processor consuming part of the algorithm and can be explained in Figures 3.10 and 3.11.

In Figure 3.10, each grid cell represents one of the raster DEM cells. θ is the angle between E (east) and L (sun azimuth). θ is derived using the AZI angle calculated in step 3. Raster pixel shown in black at point O is the initial pixel on the line along which rise and set times will be calculated. Grey pixels show the accessed pixels, which fall on the direction of line L.

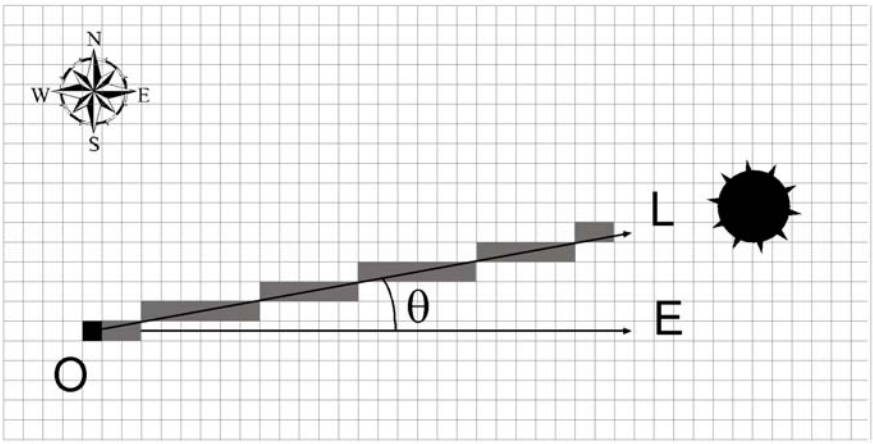

Figure 3.10: Step 4 of the sunrise calculation algorithm: accessing pixels (Plan view). Point O is the origin pixel. θ is the direction of Sun. Gray pixels indicate accessed pixels.

Once a pixel is accessed as shown in Figure 3.10, two elevation values are obtained: First one is the elevation of the origin pixel (O), second is the elevation of the accessed pixel. Using these two values together with coordinates of two pixels, the angle between pixel O and accessed pixel can be calculated over the three-dimensional topographic surface. This angle is referred to as “obstruction angle”. Thus, maximum obstruction angle on the direction of line L can be found

as each pixel is accessed. Key point here is that, the highest (most elevated) accessed pixel does not necessarily have to be the pixel causing the maximum obstruction. For example, in Figure 3.11, although point D is the highest pixel, maximum obstruction is caused by point B. Let “A” denote the accessed pixel, the following formula expresses the calculation of obstruction angle:

$$\left((Elevation)_A - (Elevation)_O\right) / \sqrt{\left((UTME)_A - (UTME)_O\right)^2 - \left((UTMN)_A - (UTMN)_O\right)^2}$$

For the sunset case, the calculation starts with the normal (unobstructed) sunset time, and iterates by decreasing this time by one minute, as it is assumed that the unobstructed set time is brought forward due to an obstruction located on the sunset direction. This time the algorithm traces towards the western horizon, as the sun sets at such azimuth angles.

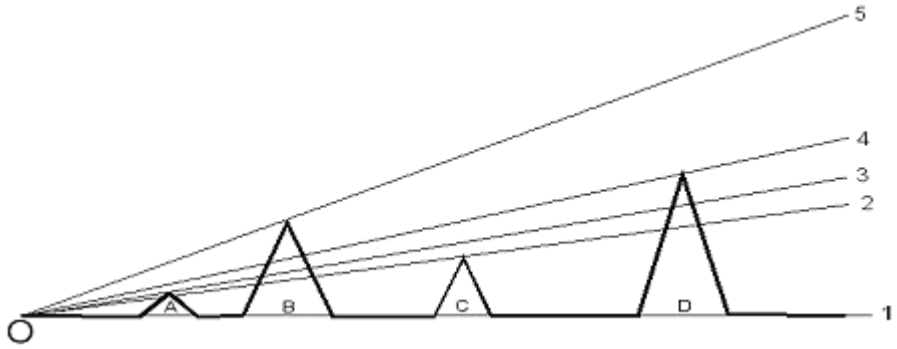

Figure 3.11: Step 4 of the sunrise calculation algorithm: finding maximum obstruction angle. Point O is the origin pixel. Points A, B, C, D indicate the obstacles.

Table 3.3 shows a sample output of the above mentioned algorithm, where UTME is the UTM easting of the pixel, UTMN is the UTM northing of the pixel, 21MAY-A is the BSD in minutes computed for 21st of May assuming there are no obstacles on the rise and set horizons (i.e. flat horizons), 21MAY-B is the BSD in minutes computed for 21st of May on a topographic surface (DEM) based on the above mentioned algorithm.

In the further analysis in this thesis, only topographically obstructed BSD values (B columns) will be taken into consideration. “A” columns, on the other hand, are calculated here since it is a part of the algorithm (step 1 above). The reason to include this column in the database is to justify that there is no change in the BSD values if topography is not included. It can be deduced from Table 3.2 that BSD time is reduced due to topographical obstructions. The amount of this reduction varies throughout the study area.

The source code of the depicted algorithm coded in ANSI C can be found in Appendix B.

Table 3.3: Sample output of the BSD calculation algorithm.

UTME	**UTMN**	**21MAY-A (no obstacles) (in minutes)**	**21MAY-B (with obstacles) (in minutes)**
436827	4489378	877	838
436827	4489478	877	839
436827	4489578	877	841
436827	4489678	877	832
436827	4489778	877	868
436827	4489878	877	865
436827	4489978	877	847
436827	4490078	877	857
436827	4490178	877	833
436827	4490278	877	838
.	.	.	.
.	.	.	.

CHAPTER 4

METHOD AND ANALYSIS

This chapter describes the method used to find the possible relationship between settlement sites and BSD. The flowchart of the method is given in Figure 4.1.

The method is composed of five successive steps. The first step is the creation of the BSD database which was partly introduced in previous chapter. The second step is the visual interpretation of this database (first section in this chapter) followed by the third step which is the removal of the unsuitable areas using topographic thresholds. This chapter ends with the fourth step of the method which seeks to investigate a relationship between the BSD and the site of the settlements. The last step of the method is the final interpretation and discussion that will be given in the next chapter.

4.1 Visual Evaluation of BSD Data

The algorithm proposed for calculation of sun times is coded in order to produce an output, which contains normal (unobstructed) total sun duration together with topographic (obstructed) total sun duration for each of the 12 months. Sample output of the program is given in Table 3.3. There are 12 files, being one for each month. 21st day of a month is chosen specifically as the day to calculate the times for a particular month, as minimum total sun time is observed on 21st of December and maximum total sun time is observed on 21st of June. An extra output column is derived using the results of previous calculations by creating a data file having a column named AVRG which contains the average value of 12 months' topographic (obstructed) BSD in minutes is also produced. A sample of this file is shown in Table 4.1.

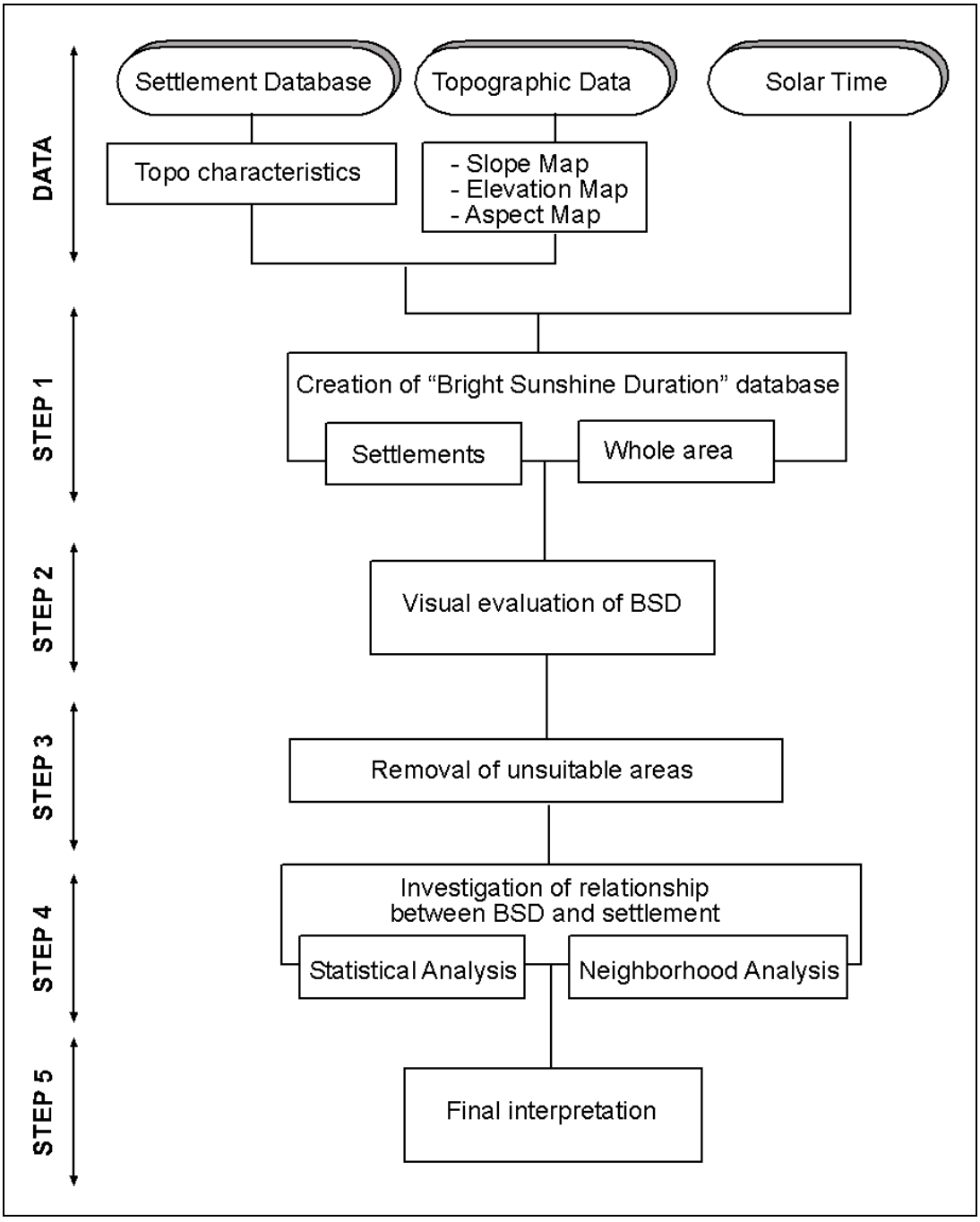

Figure 4.1: Flowchart of the method applied in this study.

Table 4.1: Sample BSD output containing average column.

UTME	UTMN	AVRG (minutes)
436827	4483473	680
436827	4483573	679
436827	4483673	675
436827	4483773	669
436827	4483873	671
436827	4483973	679
436827	4484073	687
436827	4484173	674
436827	4484273	692
436827	4484373	695
436827	4484473	696
.	.	.
.	.	.

Figure 4.2 shows the histogram of sunshine durations of 12 months, namely DEC, JAN, FEB, MAR, APR, MAY, JUN, JUL, AUG, SEP, OCT, NOV curves. This chart correlates with the cylindrical sun path diagram shown in Figure 2.9 as described below:

- December is the month having minimum BSD values
- June is the month having maximum BSD values
- Remaining 10 months are forming 5 couples as follows:

  January with November, February with October, March with September, April with August, May with July

Figure 4.3 shows the surface created by using the Kriging method on columns UTME, UTMN and AVRG. DEM of the area is also included in the figure to compare two products visually.

Figure 4.4 shows three contour maps for December, June and average of twelve months created using the Kriging method.

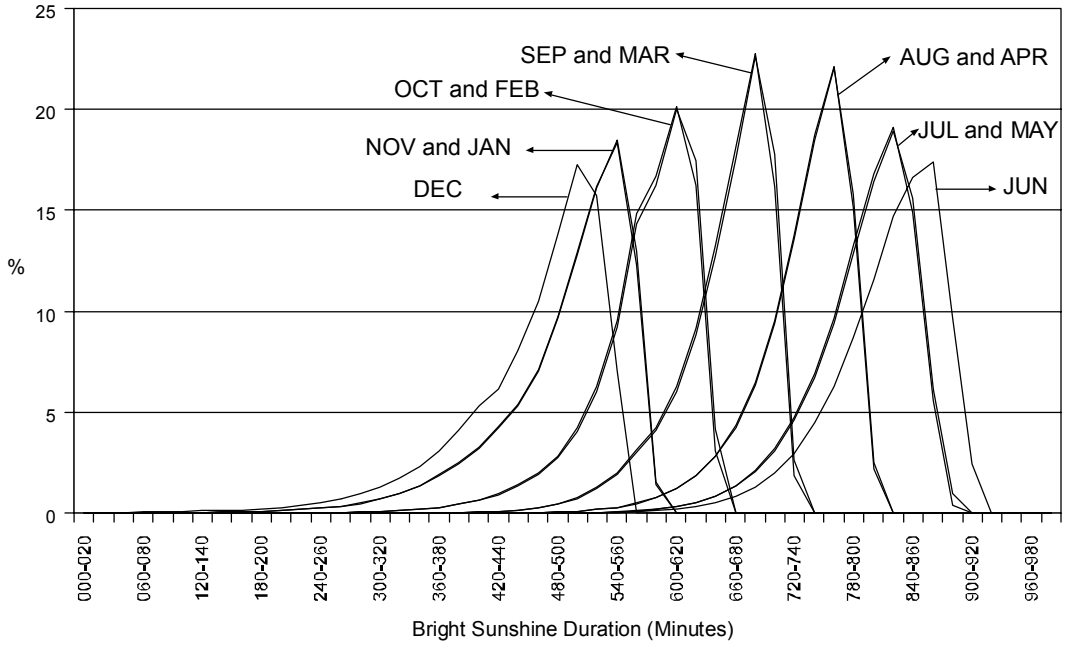

Figure 4.2: Topographic BSD histograms of 21st day of 12 months

Visual investigation of Figures 4.3 and 4.4 reveals a similarity between the elevation map of the area and these surface and contour maps. The northern part of the elevation map of the area as shown in Figure 4.3-B contains a series of mountains elongated in southeast – northwest direction and the valleys between these mountains. Pixels shown in darker colors on the northern part of the contour maps are as well elongated in SE-NW direction, thus correlating with the topographic features. Valleys between mountains are exposed to less amount of sun throughout the day. This is an expected result and is because of the obstructions caused by the mountains. Further investigating the elevation map together with the contour maps indicates that northwestern part of the elevation map has a very rough surface, and exposes concentrated darker areas. Southeastern part of the elevation map, on the other hand, contains a relatively smooth surface compared to other parts of the area, yielding to less obstruction of the sun which results in lighter areas on contour maps, meaning higher BSD values throughout the day.

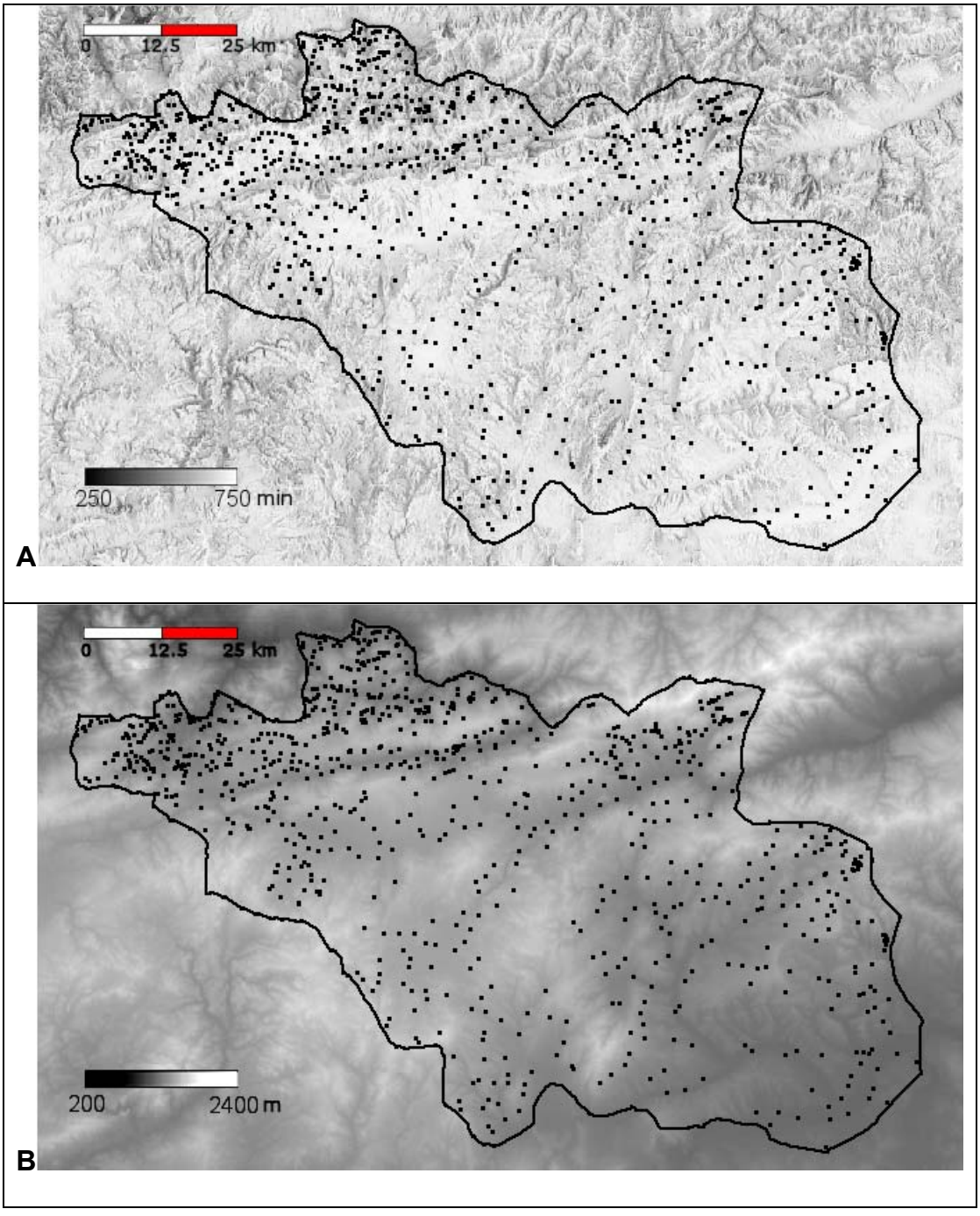

Figure 4.3: A: Average BSD surface of the study area, B: DEM of the study area. Black points indicate settlements.

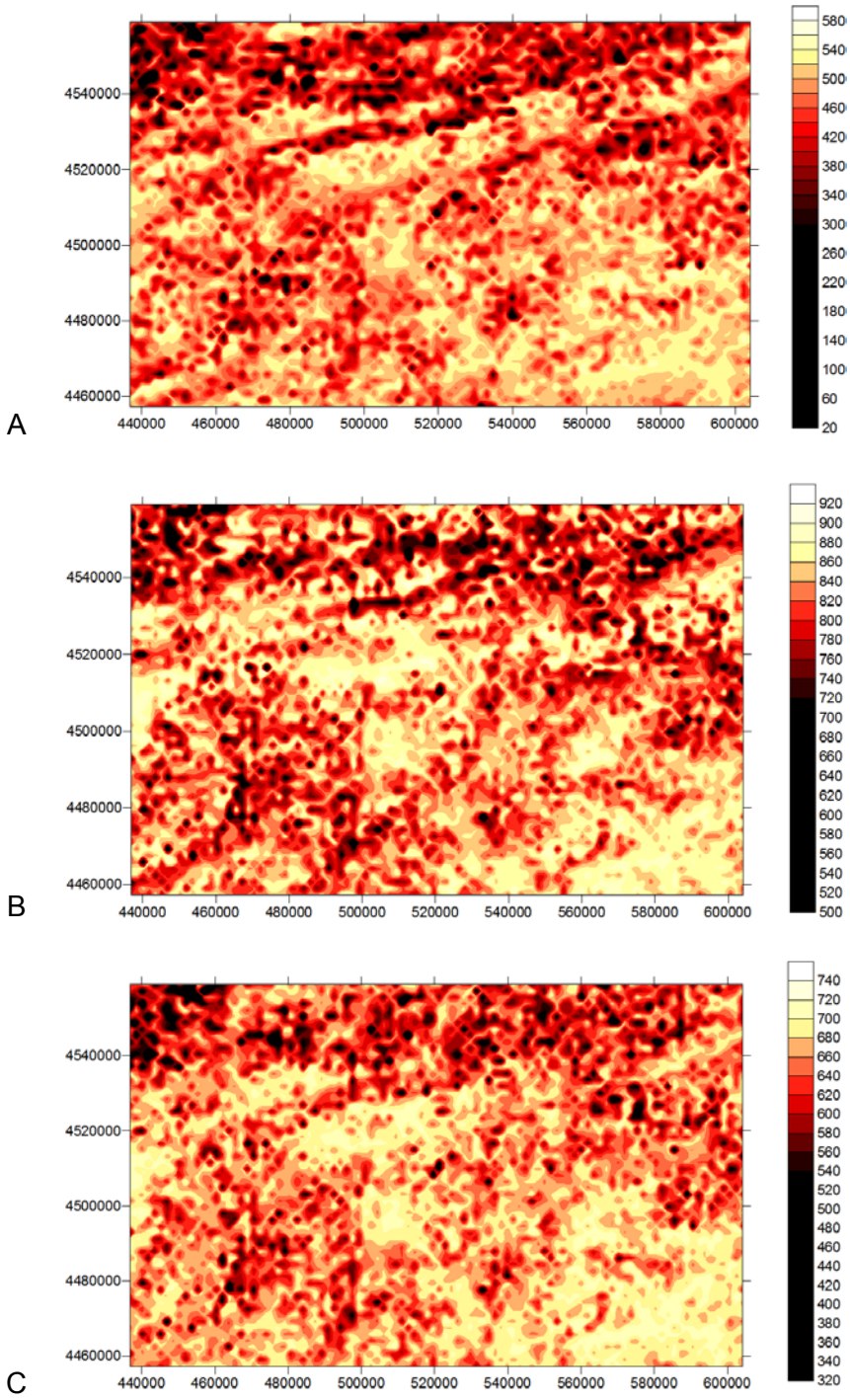

Figure 4.4: Examples of contour map showing the BSD values for December (A) June (B) and average of twelve months (C). BSD values in the scale is in minutes

4.2 Removal of Unsuitable Areas

The next step in the method is to remove the “unsuitable areas” from the study area. Unsuitable areas are defined as the areas that possess inconvenient topographic features for settlements, such as elevation, slope and aspect. These areas are less likely to be chosen as a settlement place and should be removed from the study area before starting further analysis (Özdemir, 2002; and Sürmeli, 2003).

4.2.1 Masking Analysis

Masking analysis is used for discarding unsuitable areas. To determine the thresholds in masking analysis, following steps are applied separately for each of the elevation, slope and aspect parameters:

A. Calculate the histogram of the whole study area.
B. Calculate the histogram of the settlements in the study area.
C. Subtract the histogram of the whole study area from the histogram of the settlements.
D. Determine the remove thresholds by marking negative results from previous step as “should be removed” and positive results as “should be kept”.

Figures 4.5, 4.6 and 4.7 show the results of first three steps (step A, B and C) respectively for the elevation, slope and aspect parameters. White color represents the results of step A, grey color represents the results of step B and black color represents the result of step C.

After completing steps A, B and C, three different topographic thresholds for elevation, slope and aspect can be determined by investigating the results of step C. Large negative differences between A and B (B - A) imply that areas within that topographic attribute are less likely to be chosen as a settlement place and can be discarded, whereas positive differences imply that areas within that topographic attribute are intentionally chosen as a settlement place and should be kept for further analysis.

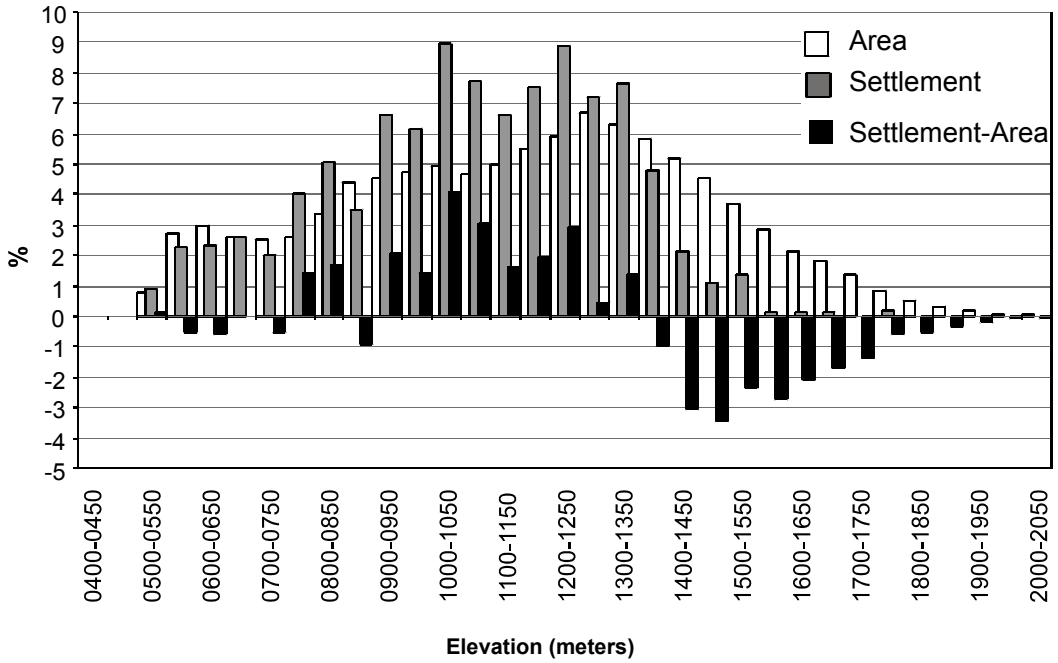

Figure 4.5: Results of Step A, B and C for the elevation parameter.

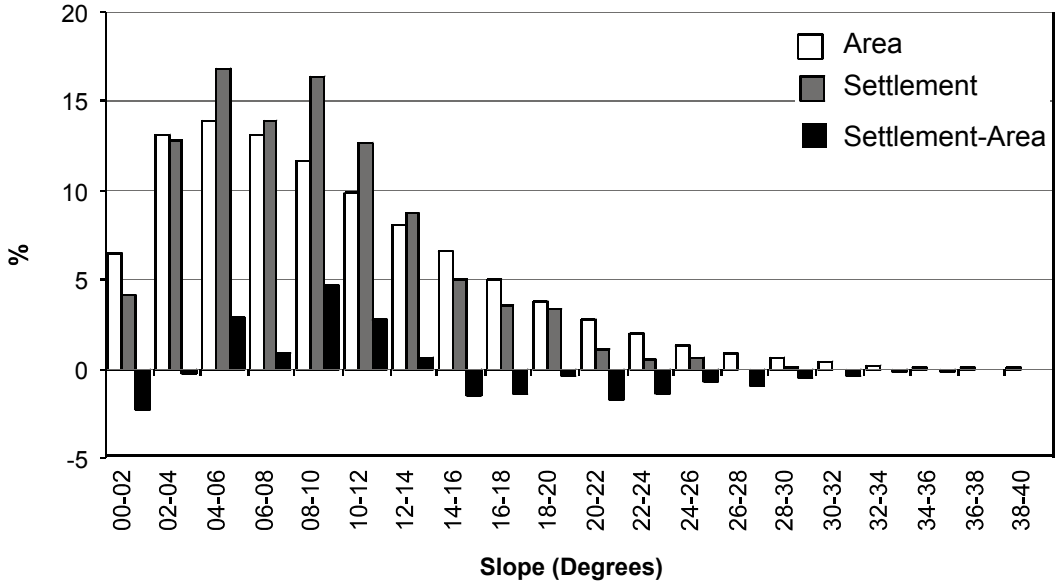

Figure 4.6: Results of Step A, B and C for the slope parameter.

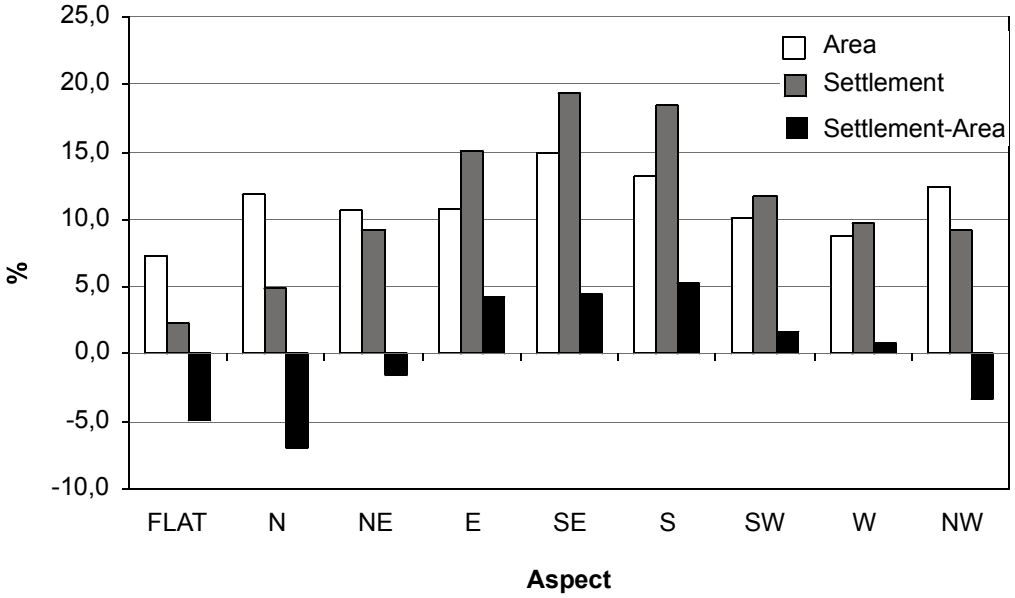

Figure 4.7: Results of Step A, B and C for the aspect parameter.

Three topographic thresholds listed in Table 4.2 are independent from each other. A pixel on the study area can be within the threshold values for elevation and slope but out of range for aspect. A total of 8 cases are possible for different combinations of these parameters. Özdemir (2002) and Sürmeli (2003)'s studies revealed that discarding areas those posses out of range values for all three topographic attributes gives the minimum (discarded settlements / discarded pixels) ratio, which yields to the most efficient way of removing unsuitable areas in proportion with discarded settlements.

Table 4.2: Topographic thresholds of masking analysis.

Topographic attribute	**Interval to be removed**	**Interval to be kept**
Elevation (m)	<750 and >1350	=>750 and =<1350
Slope (degree)	<2 and =>14	=>2 and <14
Aspect (direction)	FLAT, N, NE, NW	E, S, ES, SW, W

The algorithm used in this thesis to remove unsuitable areas is as follows:

```
If ((E < 750 or E > 1350)
and (S < 2 or S =>14)
and (A < 69 or A => 294))
{
        DISCARD;
}
else
{
        KEEP;
}
```

The output of this process is given in Figure 4.8. Black pixels indicate discarded areas and white pixels indicate remaining areas. Circles indicate discarded settlements.

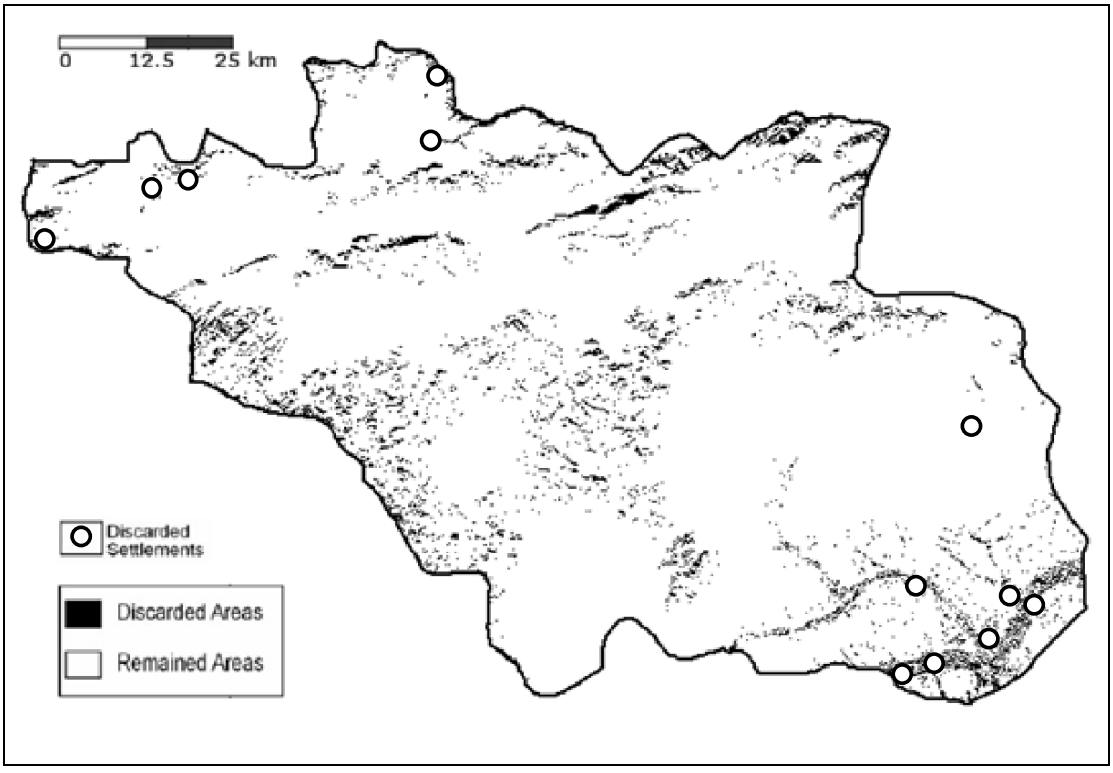

Figure 4.8: Areas and settlements discarded due to elevation, slope and aspect thresholds.

4.2.2 Evaluation of Discarded Data

Masking analysis resulted in the removal of pixels and settlements as shown in Table 4.3. Only 12 settlements out of 891 settlements (%1.34 of the settlements) have been removed, whereas %5.41 of the area is removed. The ratio between removed settlements and removed areas is 0.248 and proves that the removal method is reasonable and produces efficient results.

Table 4.3: Quantitative results of discarding operation.

Discarded Settlements		**Discarded Area**		**Ratio**
Number	Percentage	Surface(km^2)	Percentage	Settle% / Area%
12	%1.34	454.21	%5.41	0.248

Seven of the discarded settlements are in the southeastern part of the area around the Kızılırmak valley (Figure 4.8). This part of the area is characterized by low topography and flat surface. Other five settlements are in the northwestern part of the area where the region is characterized by a rough surface.

4.3 Investigation of Relationship Between Settlement Locations and BSD

In this section, remaining areas together with the remaining settlements will be analyzed to find a possible relationship between the two. This section is composed of two parts. In the first part, BSD histograms and statistics of settlements and study area will be compared for each of the twelve months and for the average of twelve months. In the second part, neighborhood analyses for the settlements are carried out by comparing the BSD values of each settlement with the BSD characteristics of a circular buffer surrounding the settlement.

4.3.1 Comparison of Histograms and Statistics

Histograms and statistics of the BSD for the study area and for the settlements are given in Figure 4.9. Each histogram represents a month of the year arranged in chronological order starting from December. Two curves in the histograms correspond to the BSD values of the study area (solid line) and BSD values of settlements (dashed line). Basic statistics of these values are illustrated in Table 4.4.

The average BSD values of all twelve months are shown in the histogram in Figure 4.10. Statistics of these values are given in Table 4.5.

Following information can be extracted by visual interpretation of these histograms and statistics:

- The BSD values are minimum in December with a mean value of 465 minutes. This value gradually increases to a maximum of 823 minutes in June. This corresponds to a BSD difference of 6 hours in a year.
- The mean BSD values of settlements and the area are very similar to each other. The difference is not more than 3 minutes in any month of the day.
- Curves in the histograms display almost similar patterns and same peak values for the area and the settlements. The only difference is the minor deflections observed in the settlements' curves.
- The minimum BSD values of the settlements are considerably higher than that of the area (Table 4.4). This is due to the N-S trending deeply dissected valleys existing in the area.

From the above 3 statements, following generalization can be made:

- Areas possessing minimum BSD values are not chosen as settlement location. Frequency of such areas, however, is very low as indicated in the histograms. General distribution of the BSD values of the settlements does not differ drastically from the distribution of the area. Therefore, the general tendency is to avoid the areas with minimum BSD values.

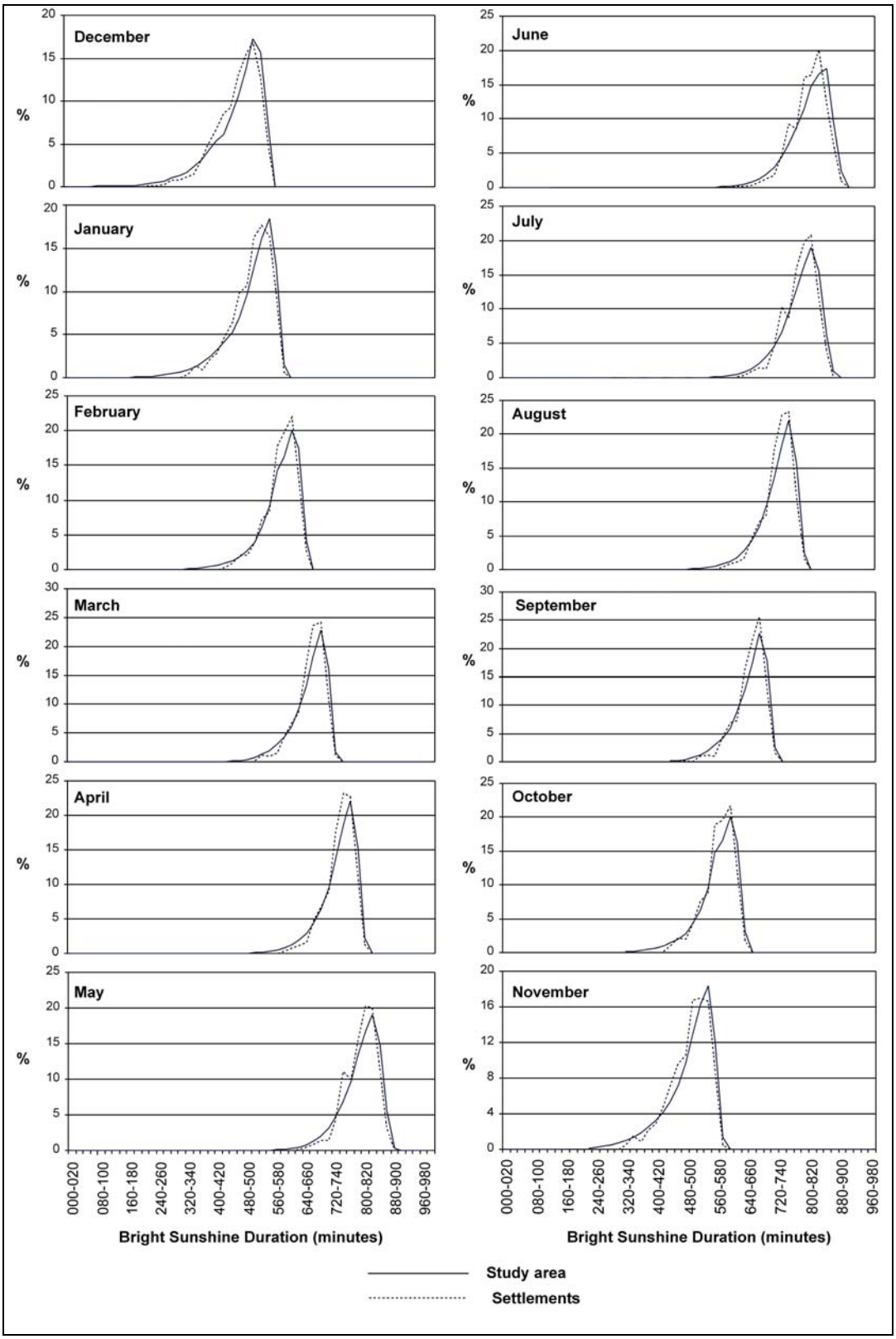

Figure 4.9: BSD histograms of the area and settlements for 12 months.

Table 4.4: BSD statistics of the study area and settlements for 12 months.

Month	Region	Minimum (minutes)	Maximum (minutes)	Range (minutes)	Mean (minutes)	Std. Dev. (minutes)
December	**Whole Area**	16	558	542	464.9	73.1
	Settlements	239	554	315	467.1	57.1
January	**Whole Area**	20	588	568	499.5	67.8
	Settlements	325	583	258	502.8	51.5
February	**Whole Area**	56	657	601	577.5	54.1
	Settlements	420	653	233	580.3	41.7
March	**Whole Area**	168	732	564	657.5	49.3
	Settlements	463	729	266	660.3	39.6
April	**Whole Area**	318	815	497	737.2	48.8
	Settlements	539	813	274	739.4	39.3
May	**Whole Area**	367	881	514	797.2	52.2
	Settlements	578	879	301	796.8	43.2
June	**Whole Area**	393	909	516	823.6	54.7
	Settlements	582	908	326	820.9	46.3
July	**Whole Area**	368	883	515	799.0	52.4
	Settlements	579	881	302	798.4	43.3
August	**Whole Area**	319	816	497	738.0	48.9
	Settlements	540	814	274	740.2	39.3
September	**Whole Area**	167	734	567	659.6	49.3
	Settlements	463	731	268	662.5	39.5
October	**Whole Area**	55	655	600	575.2	54.3
	Settlements	416	651	235	578.1	41.7
November	**Whole Area**	21	587	566	498.4	68.0
	Settlements	323	582	259	501.7	51.7

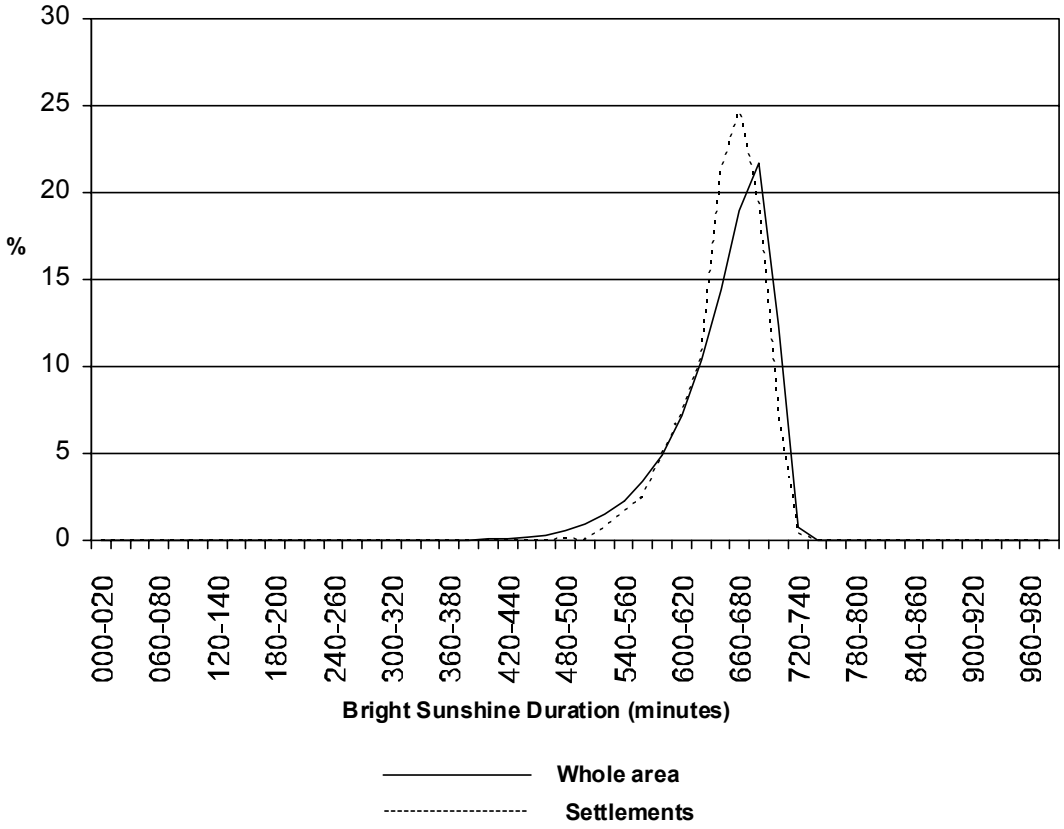

Figure 4.10: BSD histograms of the study area and settlements for the average of 12 months.

Table 4.5: BSD statistics of the study area and settlements for the average of 12 months.

(minutes)	Minimum	Maximum	Range	Mean	Std. Dev.
Whole Area	265	732	467	651.8	49.7
Settlements	492	722	230	653.6	38.3

4.3.2 Neighborhood Analysis

Histograms presented in the previous section can only suggest on the distribution of the area and the settlements against the BSD values and give a general idea on the relationship between the two. However, the relative location of the settlement within the BSD surface is not predicted in these diagrams. The distances, for example, to the nearest maximum and minimum BSD values are not known (Figure 4.11). For this purpose, a particular analysis on settlements should be carried out that will locate the site of settlement in relation to the nearest local extreme points in a given circular buffer area.

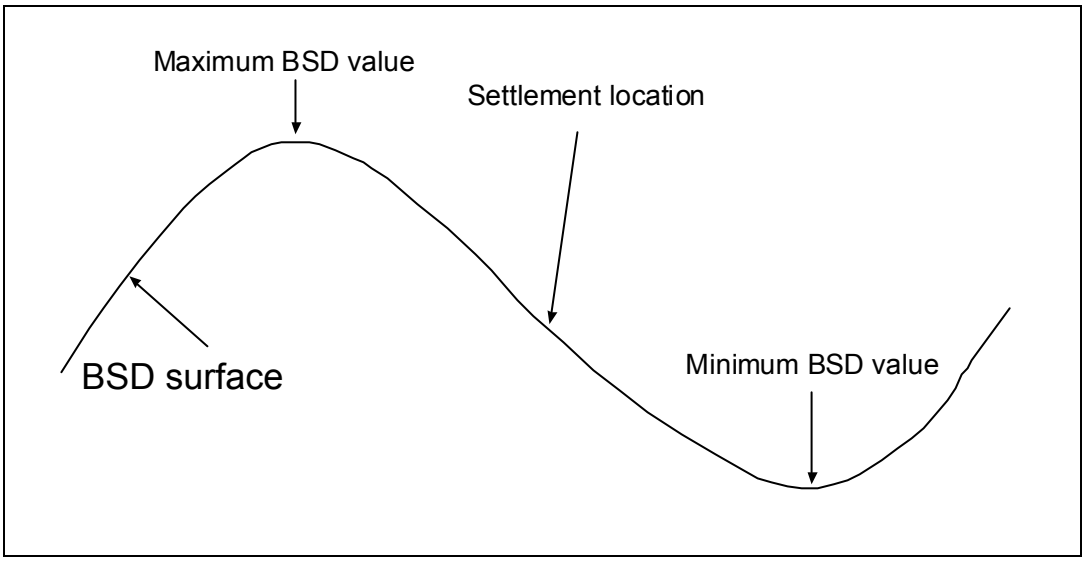

Figure 4.11: A BSD surface illustrating the location of a settlement in relation to the nearest local maximum and minimum BSD values

In this respect, a radius of the circular buffer area around each settlement should be selected. This radius could be calculated from the variation of the BSD surface. To investigate this variation, four profiles elongated in E-W direction are drawn over the average BSD surface as illustrated in Figure 4.12.

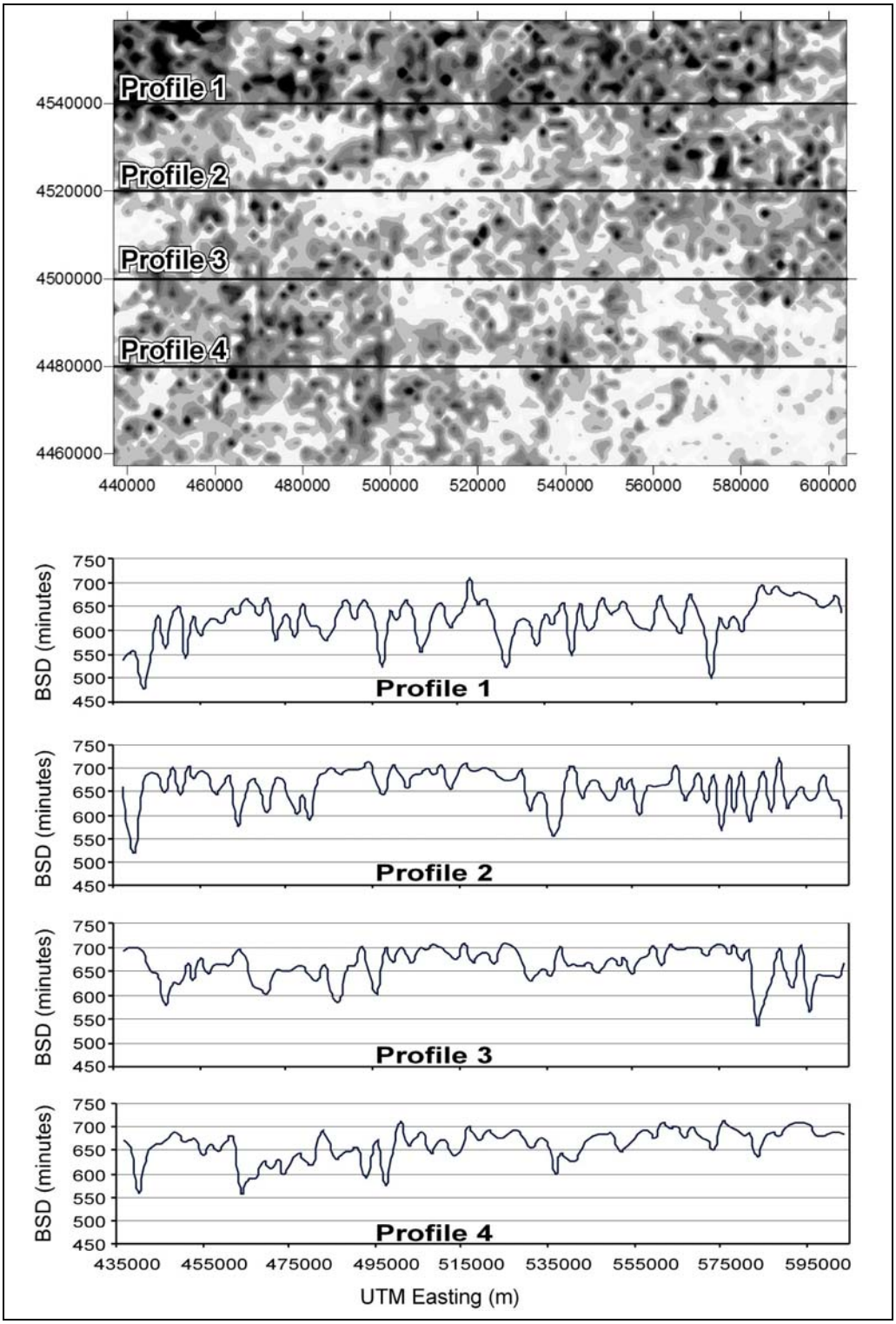

Figure 4.12: Four profiles over BSD surface to derive the radius of the circular buffer area. Frequency of crests or troughs is considered to estimate the radius.

The frequency of crests (or troughs) is divided to the length of profile to obtain the average wavelength over the surface (Table 4.6). Therefore the diameter of the buffer is equal to the wavelength and the radius should be half of this value. The average wavelength is approximately 5 kms.

Table 4.6: Results of profile process for radius determination of buffer area.

Profile	# of Crests (or troughs)	Profile Length	Average Wavelength
1	32	165 km	5.15 km
2	34	165 km	4.85 km
3	35	165 km	4.71 km
4	31	165 km	5.32 km

For each settlement following information is needed for the analysis:

- BSD value of the settlement
- BSD values of extreme pixels within the buffer area
    - Minimum BSD value
    - Maximum BSD value
- Distance to extreme pixels within the buffer area
    - Distance to pixel having minimum BSD value
    - Distance to pixel having maximum BSD value
- Average BSD value of the buffer area

To obtain this information, a simple program, which calculates the above parameters by accessing the surrounding pixels in the buffer area, is coded. Using these parameters, two different comparisons are made:

- Analyzing the “distance to pixel having minimum BSD value” and “distance to pixel having maximum BSD value”.
- Analyzing the “BSD value of the settlement” with minimum, maximum and average BSD value of the buffer area.

4.3.2.1 Analysis of Distance to Minimum BSD Pixel and Distance to Maximum BSD Pixel

The analysis is based on the comparison of the distance to minimum BSD value with the distance to maximum BSD value in order to find out whether the settlement is in tendency of moving towards the area that has the maximum BSD value. In Figure 4.13, settlement is indicated with “O”, the pixel having minimum BSD value is indicated with “m” and the pixel having maximum BSD value is indicated with “M”. |Om| is the distance to pixel having minimum BSD, |OM| is the distance to pixel having maximum BSD.

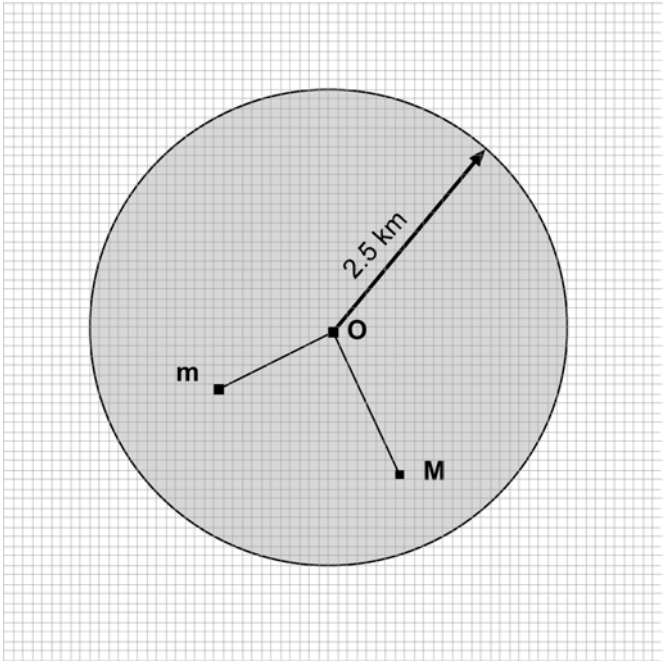

Figure 4.13: Distance to minimum BSD pixel (|Om|), distance to maximum BSD pixel (|OM|)

Histograms of “distance to minimum BSD pixel” and “distance to maximum BSD pixel are given in figure 4.14.

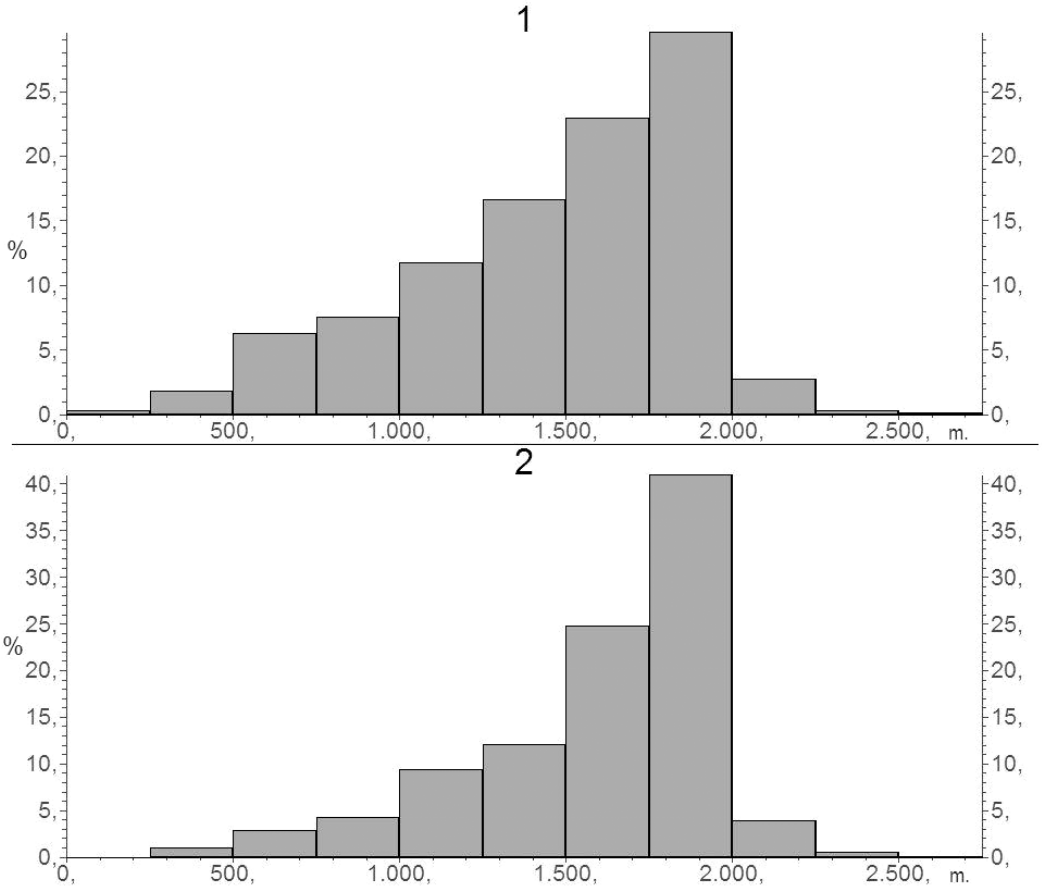

Figure 4.14: A: Settlements’ distance to minimum BSD pixel histogram, B: Settlements’ distance to maximum BSD pixel histogram.

Figure 4.15 shows the histogram of distance to minimum BSD pixel / distance to maximum BSD pixel (|OM| / |Om|) ratio. The range of the ratio is between 0.19 and 6.64.

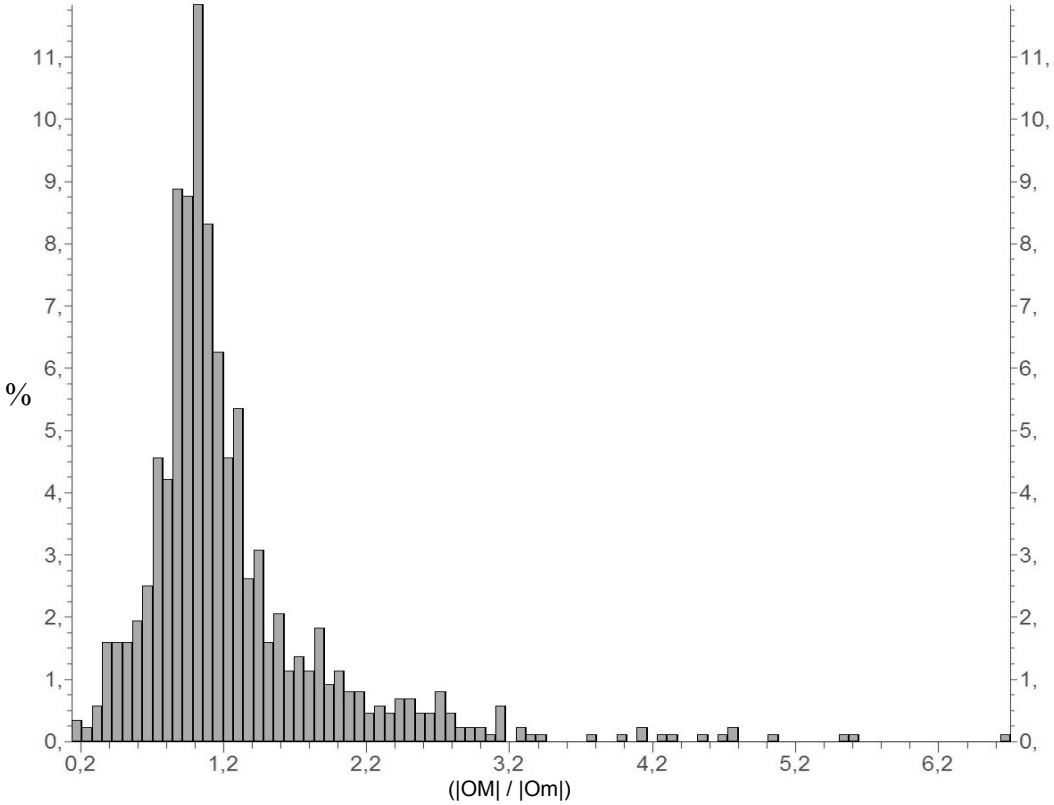

Figure 4.15: Histogram of (|OM| / |Om|) as illustrated in Figure 4.13.

Following simple algorithm is applied to compare |Om| and |OM| distances:

IF 0 =< (|OM| / |Om|) < Minimum Threshold
    Closer to maximum BSD pixel
ELSE
IF Minimum Threshold =< (|OM| / |Om|) =< Maximum Threshold
    Relatively equi-distance
ELSE
IF Maximum Threshold < (|OM| / |Om|)
    Closer to minimum BSD pixel

Table 4.7 lists the results of the above algorithm respectively for three threshold pairs: 1st pair = 0.7 – 1.3, 2nd pair = 0.8 – 1.2, 3rd pair = 0.9 – 1.1. It can be deduced from Table 4.7 that as the difference between minimum threshold and

maximum threshold decreases, percentage of settlements located closer to maximum BSD pixel and percentage of settlements located closer to minimum BSD pixel increases. Expectedly, percentage of settlements located relatively equi-distance to minimum and maximum BSD pixels decreases. However, none of the three threshold pairs indicates a strong evidence about the relationship between settlement location and BSD by means of comparing the two distances.

Table 4.7: Settlement percentage for distance analysis with different thresholds (T.).

	% of settlements located closer to max. BSD pixel	% of settlements located relatively equi-distance	% of settlements located closer to min. BSD pixel
Min. T.=0.7 Max. T.=1.3	%10.2	%60.4	%29.4
Min. T.=0.8 Max. T.=1.2	%15.7	%48.5	%35.8
Min. T.=0.9 Max. T.=1.1	%25.4	%29.4	%45.2

4.3.2.2 Analysis of BSD Value of the Settlement and BSD Values of the Buffer Area

BSD values of the settlements are compared with the statistical parameters of the BSD values of buffer areas. Figure 4.16 shows the histograms of minimum BSD, maximum BSD values of the buffer zones and BSD values of settlements. Total number of data in each histogram is 879 (12 was discarded).

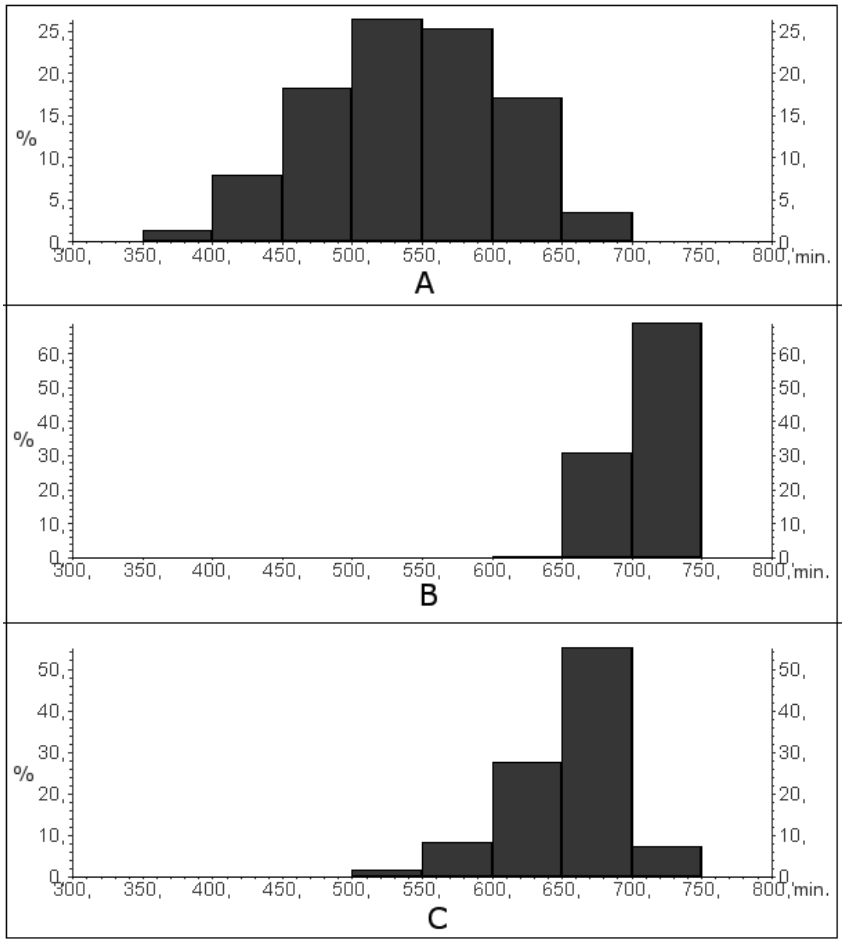

Figure 4.16: A: Minimum BSD values of buffer areas histogram, B: Maximum BSD values of buffer areas histogram, C: Settlements BSD values histogram

It can be deduced from Figure 4.16 that majority of the settlements have avoided settling on landforms having lower BSD values. In other words, they have a tendency to settle towards landforms having higher BSD values.

Figure 4.17 shows the histograms of settlement's BSD and buffer's average BSD. These two histograms at first sight seem to have similar distributions. The ratio of (settlement's BSD / buffer's average BSD) can be used to extract definite results by rationing the two histograms. Figure 4.18 shows the histogram of (settlement's BSD / buffer's average BSD) ratio. The range of the ratio is between 0.84 and 1.14.

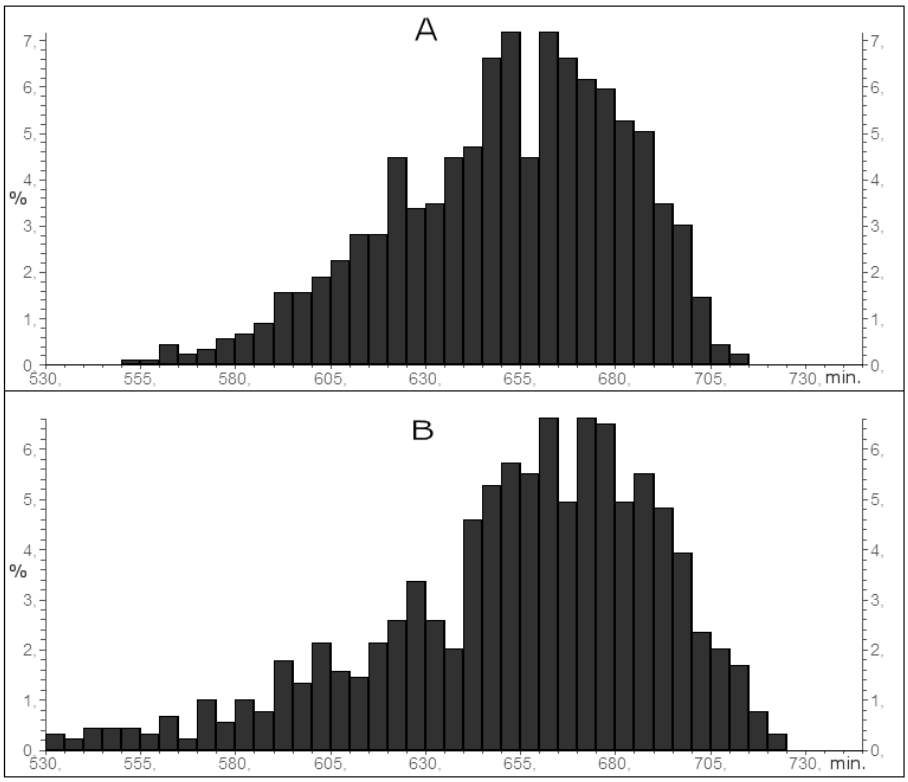

Figure 4.17: A: Average BSD of the buffer areas histogram, B: Settlements BSD histogram

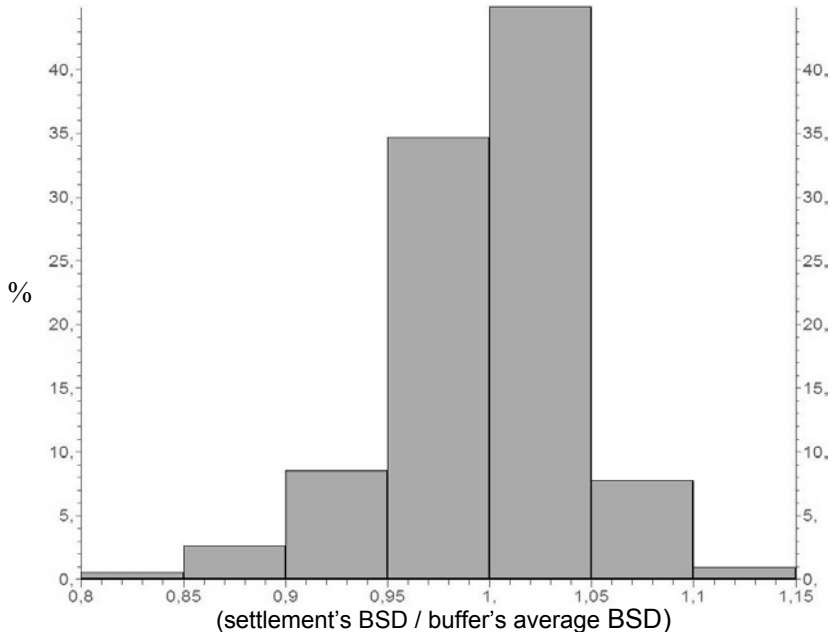

Figure 4.18: Histogram of (settlement's BSD / buffer's average BSD) ratio

Following simple algorithm is applied for grouping the settlements into three categories:

IF 0 =< (BSD(Settlement) / AverageBSD(Buffer)) < Minimum Threshold

Settlement has a lower BSD

ELSE

IF Minimum Threshold =< (BSD(Settlement) / AverageBSD(Buffer)) =< Maximum Threshold

Settlement has almost equal BSD

ELSE

IF Maximum threshold < (BSD(Settlement) / AverageBSD(Buffer))

Settlement has a greater BSD

Table 4.8 lists the results of the above algorithm respectively for two threshold pairs: 1st pair = 0.9 – 1.1, 2nd pair = 0.95 – 1.05.

This analysis shows that most of the settlements (%96.7 in the first threshold pair, %83.8 in the second threshold pair) have almost the same average BSD values of their buffer zones. Rest of the settlements has, more or less, similar percentages above or below the average BSD values of their buffer zones.

Table 4.8: Settlement percentages with respect to their buffer zones' average BSD value (for two different threshold pairs).

	% of settlements having lower BSD	% of settlements having almost equal BSD	% of settlements having greater BSD
Min. T.=0.9 Max. T.=1.1	%2.4	%96.7	%0.9
Min. T.=0.95 Max. T.=1.05	%7.5	%83.8	%8.7

CHAPTER 5

DISCUSSION

In this chapter three aspects of the thesis will be discussed. These are 1) methodology of the study, 2) the data used in this study, and 3) results obtained with this methodology.

5.1 Methodology

The methodology applied in this study is simple and straightforward. In general the method considers following aspects:

- The most important input data is topographic surface. A DEM data having 100 m cell size is used provided by SRTM.
- A program is written that calculates sunrise and sunset times using DEM. These data are used to produce a BSD surface of the study area.
- Unsuitable landforms for settlement are clipped out from the study area. The thresholds during this process are derived from elevation, slope and aspect parameters of the settlements located within the area using topographic characteristics of the study area.
- The first step in the analysis is comparison of BSD histograms and statistics of settlements and study area. This comparison is performed for each of the twelve months and for the average of twelve months.
- The next step is the neighborhood analysis, which is carried out for the settlements by comparing the BSD values of each settlement with the BSD characteristics of a circular buffer surrounding the settlement.

Following aspects, however, could be considered in the method that might increase the accuracy of the results.

Consideration of obstruction: This study considers that two main obstructions exist only in the eastern (sunrise) and western (sunset) directions. For this reason, other obstructions that might exist in various directions should be taken into account, particularly in the southern direction due to the path of the sun.

Other factors influencing BSD data: Since the main purpose of the production BSD data is to emphasize the effect of topography on sunrise-set times, all other external parameters should also be included in the calculations. Some parameters that may affect the BSD are as follows:

- Effect of atmospheric refraction caused by the nature of atmosphere
- Effect of cloud cover present on the atmosphere

Effect of atmospheric refraction should be further analyzed and modeled by using physical and astronomical rules.

It might be difficult to model the cloud cover since it cannot be easily predicted throughout the year and it might be difficult to obtain the cloud cover data. In case of such difficulties, the method could be applied only for the summer months since cloud cover is barely observed and has a minimum effect on BSD.

Selection of thresholds: Thresholds are used in removal of unsuitable areas. Non-preferred intervals of elevation, slope and aspect are discarded according to thresholds calculated using settlement data and the study area. Selection of thresholds is area dependable and may vary in different regions with different settlement pattern and topographic surface.

Application to different study areas: Although Çankırı is selected as the study area, the methodology and the program written in this thesis can as well be applied to another region provided that the initial data used in the study is made available for the selected region.

5.2 Data Used

Regarding the data used in this study, following issues can be of further discussion:

Preparation of BSD data: BSD data was not available before this study. Therefore, BSD data is calculated by a specifically tailored algorithm, which is based on the document titled “General Solar Position Calculations” supplied by NOAA. This document formulates the calculation of unobstructed sunrise and sunset times. However, this thesis emphasizes the effect of the topography on sunrise and sunset times and needs the obstructed times. Therefore, a new algorithm taking the effect of topography into consideration is built up on the basis of the NOAA formulations.

Resolution of DEM data: DEM data used in this study had a cell size of 100 meters. This resolution is believed to be the optimal solution since it is reasonable to obtain BSD values for each 100 meters considering the size of the area included in the study. A finer grid size should give a more detailed view about the surface; however, this increases the number of pixels and requires much more time for sun duration calculation algorithms to finish.

Vertical accuracy of DEM data: The vertical accuracy of SRTM DEM data is 16 meters. Since this study is based on using DEM values, it is important to obtain an accurate data to produce accurate results. There are some other sources of DEM data available from different suppliers, some of which having better accuracy.

Settlement data: Each settlement is represented by a point vector data. These points are probably the initial points of the settlements. Normally, a settlement occupies an area on the landform and might also be represented by a polygon. Representing a settlement by a point is more convenient since effect of BSD in selecting the initial settlement location is investigated in this study.

5.3 Results Obtained

Results of the analysis that investigate the relationship between settlement location and BSD are illustrated in histograms and tables in section 4.3. The results do not indicate a strong relationship as shown particularly in Figures 4.9 and 4.10. Overall BSD values of the study area and the settlements display similar patterns.

Further analyses are carried out to investigate whether the BSD value changes as the location of the settlement moves. For this reason four profiles are measured to obtain the nature of the variation over the BSD surface. This variation is used as radius for the neighborhood analysis. This analysis shows that the BSD value does not change as the settlement location changes within the buffer zone. Most of the settlements have almost the same average BSD values of their buffer zones. Rest of the settlements has, more or less, similar percentages above or below the average BSD values of their buffer zones.

CHAPTER 6

CONCLUSIONS

The main conclusion of this thesis is that there is not an obvious relationship between the location of the settlement and bright sunshine duration (BSD). Accordingly, BSD is not an important factor on the selection of a settlement site. Other factors investigated for the same area, on the other hand, indicate that there is a considerable effect of certain parameters on the location of settlements. For example, morphological landform (Sürmeli, 2003) and rock type (Özdemir, 2002) played an important role for the selection of a site. This role for the BSD, however, is not observed for Çankırı province.

REFERENCES

Bradford M.A.C., 2001, Caribbean Perspectives on Settlement Patterns: The Windward Island Study, Ph.D. Thesis, The University of IOWA, United States

Hofierka J., **Suri M.**, The Solar Radiation Model for Open Source GIS: Implementation and Applications**,** Proceedings of the Open source GIS - GRASS users conference 2002 - Trento, Italy, 11-13 September 2002

Hunt E.D., 1990, A Consideration of Environmental, Physiographic and Horticultural Systems as They Impact Late Woodland Settlement Patterns in Western New York State: A Geographic Information System (GIS) Analysis of Site Location, Ph.D Thesis, State University of New York at Buffalo, United States

Keller C., **Hall J.K.**, 1999, Using a Digital Terrain Model to Calculate Visual Sunrise and Sunset Times, Computers & Geosciences 26 (2000) pp. 991-1000

Kuiper A.J., **Wescott K.L.**, 1999, A GIS Approach for Predicting Prehistoric SiteLocations. Presented at the Nineteenth Annual ESRI User Conference, San Diego, California, USA, July 26-30, Sponsored by ESRI

Kumar L., Skidmore A.K., Knowles E., 1997, Modelling Topographic Variation in Solar Radiation in a GIS Environment. International Journal of Geographical Information Science 11, pp. 475-97

Lourens E.M.J., 1994, The application of a Geographical Information System to Identify Areas Suitable for Urban Settlement, M.Sc. Thesis, University of Pretoria, South Africa

Maizel M., 2003, Historical Interrelationships Between Population Settlement and Farmland in the Conterminous United States, 1790 to 1992, USGS Land Use History of North America Program

Mazria E., 1979, The Passive Solar Energy Book, Rodale Press

NASA, 1999, Solar Insolation Key Concepts, http://education.gsfc.nasa.gov/experimental/July61999siteupdate/inv99Project.Site/Pages/solar.insolation.html (last accessed: 14-Aug-2004)

NASA SRTM, 2004, Shuttle Radar Topography Mission, http://www2.jpl.nasa.gov/srtm/ (last accessed: 14-Aug-2004)

Nelson R.R., 2000, Introduction to Geographic Data Analysis, University College of the Cariboo, Canada, http://www.cariboo.bc.ca/ae/ses/geog/Courses/270/text/G270/text/G20-04.PDF (last accessed: 14-Aug-2004)

NOAA glossary, 2004, Astronomical Terms, http://www.srh.noaa.gov/ffc/html/gloss3.shtml (last accessed: 14-Aug-2004)

Noss, R.F., 1985, Spatial Distribution of Resources and Human Settlement and Foraging in the Alaska Yukon River Valley, Ph.D. Thesis, University of Florida, United States

Özdemir, T., 2002, A GIS Approach to Investigate the Relationship Between Original Settlement and Rock Type Utilizing Topography with an Application to Çankırı Province, M.Sc. Thesis, Middle East Technical University, Turkey

Stea D., **Turan M.**, 1993, Placemaking, Avebury Press

Sürmeli B.G., 2003, Relationship Between Settlement Location And Morphological Landform: A GIS Method Applied to Çankırı Province, M.Sc. Thesis, Middle East Technical University, Turkey

APPENDIX A

GENERAL SOLAR POSITION CALCULATIONS FROM NOAA

1) Fractional year, in radians.

$$\gamma = \frac{2\pi}{365} * (day\_of\_year - 1 + \frac{hour - 12}{24})$$

day_of_year: current day of year..

hour: Current hour of day.

2) Equation of time, in minutes.

$$eqtime = 229.18 * (0.000075 + 0.001868\cos\gamma - 0.032077\sin\gamma - 0.014615\cos 2\gamma - 0.040849\sin 2\gamma)$$

γ: fractional year, in radians.

3) Solar declination angle, in radians.

$$decl = 0.006918 - 0.399912\cos\gamma + 0.070257\sin\gamma - 0.006758\cos 2\gamma + 0.000907\sin 2\gamma - 0.002697\cos 3\gamma + 0.00148\sin 3\gamma$$

γ: fractional year, in radians.

4) Time offset, in minutes.

$$time\_offset = eqtime - 4 * \text{longitude} + 60 * \text{timezone}$$

longitude: longitude, in degrees.

timezone: time zone, in hours.

5) True solar time, in minutes.

$$tst = hr * 60 + mn + sc / 60 + time\_offset$$

hr: hours (0 - 23).

mn: minutes (0 - 60).

sc: seconds (0 - 60).

6) Solar hour angle, in degrees.

$$ha = (tst / 4) - 180$$

tst: true solar time, in minutes.

7) Solar zenith angle (ϕ) can be found from the following equation.

$$\cos\phi = \sin(lat)\sin(decl) + \cos(lat)\cos(decl)\cos(ha)$$

8) Solar azimuth (θ, clockwise from north) can be found from the following equation.

$$\cos(180 - \theta) = -\frac{\sin(lat)\cos\phi - \sin(decl)}{\cos(lat)\sin\phi}$$

Sunrise Sunset Calculations

For the special case of sunrise or sunset, the zenith is set to 90.833° (the approximate correction for atmospheric refraction at sunrise and sunset), and the hour angle becomes:

$$ha = \pm \arccos\left(\frac{\cos(90.833)}{\cos(lat)\cos(decl)} - \tan(lat)\tan(decl)\right)$$

where the positive number corresponds to sunrise, negative to sunset.

Then the UTC time of sunrise (or sunset) in minutes is:

$$sunrise = 720 + 4(longitude - ha) - eqtime$$

longitude: longitude, in degrees.

ha: hour angle, in degrees.

eqtime: equation of time, in minutes.

APPENDIX B

ALGORITHM/CODE FOR SUNRISE-SUNSET AND BSD CALCULATION OVER A TOPOGRAPHIC SURFACE USING DEM

```
/* Routines for Sunrise-Sunset and BSD calculation over DEM
   Emre Erdogan, 2004, METU
*/

#include <stdio.h>
#include <alloc.h>
#include <math.h>
#include "convert.h"

#define dtr ( M_PI / 180.0)
#define rtd  (180.0 / M_PI)

#define YEAR_LENGTH 365
#define RISESET_ZENITH 90.833
#define TIME_ZONE 2

#define ROWS 1176
#define COLS 1993
#define CELL_SIZE 100

#define N_DOWN_LEFT 4449344.081
#define E_DOWN_LEFT 420819.240
#define N_UP_RIGHT 4566944.081
#define E_UP_RIGHT 620119.240
#define N_UTM_RANGE (N_UP_RIGHT - N_DOWN_LEFT)
#define E_UTM_RANGE (E_UP_RIGHT - E_DOWN_LEFT)
#define UTMZONE "36T"

int monthdays[13] ={0,31,59,90,120,151,181,212,243,273,304,334,365};

struct mydate
{
   int year;
   int month;
   int day;
};

struct mytime
{
   int hour;
```

```
  int minute;
};

FILE *infile, *outfile;

int *fptr;

struct point_data
{
  int x, y, elev;
};

double d2r (double deg)
{
  return
    (deg / 180.0) * M_PI;
}

double r2d (double rad)
{
  return
    (rad / M_PI) * 180;
}

double fractional_year (int dayofyear)
{
  return ((2 * M_PI) / YEAR_LENGTH) * dayofyear;
}

double equation_of_time (double fractyear)
{
  return
    229.18 *
    (
          0.000075
          + 0.001868 * cos(fractyear)
          - 0.032077 * sin(fractyear)
          - 0.014615 * cos(2 * fractyear)
          - 0.040849 * sin(2 * fractyear)
    );
}

double declination_angle (double fractyear)
{
  return
    (
         0.006918
         - 0.399912* cos(fractyear)
         + 0.070257* sin(fractyear)
         - 0.006758* cos(2 * fractyear)
         + 0.000907* sin(2 * fractyear)
         - 0.002697* cos(3 * fractyear)
         + 0.00148*  sin(3 * fractyear)
    );
}
```

```
double time_offset (double eqtime, double longitude)
{
  return
    eqtime - (4 * -longitude) + (60 * -TIME_ZONE);
}

double true_solar_time (int hr, int mn, int sc, double tos)
{
  return
    (hr * 60) + mn + (sc/60) + tos;
}

double solar_hour_angle (double tst)
{
  return
    (tst / 4) - 180;
}

double zenith_angle (double lat, double decl, double ha)
{
  return
    acos
    (
        (sin(dtr*lat) * sin(decl)) + (cos(dtr*lat) * cos(decl) * cos(dtr*ha))
    );
}

double azimuth_angle (double lat, double zen, double decl)
{
  return
    acos
    (
        ((sin(dtr*lat) * cos(dtr*zen)) - sin(decl)) /
        (cos(dtr*lat) * sin(dtr*zen))
    );
}

double hour_angle_rise (double lat, double decl, double zen)
{
  double correction =
        ( cos(dtr*zen) / (cos(dtr*lat) * cos(decl)) )
         - (tan(dtr*lat) * tan(decl));

  if (correction > 1) return 0;
  else if (correction < -1) return M_PI;
  else return acos(correction);

}

double hour_angle_set (double lat, double decl, double zen)
{
  return
    - hour_angle_rise (lat, decl, zen);
}
```

```
double sun_in_minutes (double lon, double hourangle, double eqtime)
{
  return
    720 + 4 * (-lon - rtd*hourangle) - eqtime;
}

struct mytime calc_rise_set (int dayofyear, double lat, double lon, double zen, int set)
{
  double minutes, ha, frac, eqtime, decl;
  struct mytime risesettime;

  frac = fractional_year(dayofyear);
  eqtime = equation_of_time(frac);
  decl = declination_angle(frac);

  if (set)
    ha = hour_angle_set(lat, decl, zen);
  else
    ha = hour_angle_rise(lat, decl, zen);

  minutes = sun_in_minutes (lon, ha, eqtime);
  risesettime.hour = (int) minutes / 60;
  risesettime.minute = (int) minutes % 60;
  return risesettime;
}

int day_of_year (struct mydate indate)
{

  return monthdays[indate.month-1] + indate.day;
}


int get_point (int x, int y)
{
  int mem_y;

  mem_y = ROWS - y - 1;
  return fptr[mem_y * COLS + x];
}

double find_zenith_angle (struct point_data pt1, struct point_data pt2)
{
  return
   M_PI_2 -
   atan (
     (pt2.elev - pt1.elev)  /
     (CELL_SIZE *
     (sqrt((pt2.x-pt1.x)*(pt2.x-pt1.x) + (pt2.y-pt1.y)*(pt2.y-pt1.y))))
   );
}

struct point_data trace_for_sunrise (int x, int y, double angle)
{
```

```
  int deltay, i, j;
  double minzenithangle = M_PI;
  struct point_data startpoint, tracepoint, minzenithpoint;

  startpoint.x = x;
  startpoint.y = y;
  startpoint.elev = get_point (x ,y);

  for (i=x+1, j=1; (i < COLS) && (j<200); i++, j++)
  {
    if (angle > 0.0) deltay = (int) ((j * tan (angle) + 0.5));
    else deltay = (int) ((j * tan (angle) - 0.5));
    if ((y + deltay >= 0) && ( y + deltay < ROWS))
    {
      tracepoint.x = i;
      tracepoint.y = y + deltay;
      tracepoint.elev = get_point (i, y + deltay);
      if (find_zenith_angle(startpoint, tracepoint) < minzenithangle)
      {
        minzenithangle = find_zenith_angle(startpoint, tracepoint);
        minzenithpoint.x = i;
        minzenithpoint.y = y + deltay;
        minzenithpoint.elev = tracepoint.elev;
      }
    }
  }

  return minzenithpoint;
}

struct point_data trace_for_sunset (int x, int y, double angle)
{
  int deltay, i, j;
  double minzenithangle = M_PI;
  struct point_data startpoint, tracepoint, minzenithpoint;

  startpoint.x = x;
  startpoint.y = y;
  startpoint.elev = get_point (x ,y);

  for (i=x-1, j=1; (i >= 0) && (j<200); i--, j++)
  {
    if (angle > 0.0) deltay = (int) ((j * tan (angle) + 0.5));
    else deltay = (int) ((j * tan (angle) - 0.5));
    if ((y + deltay >= 0) && ( y + deltay < ROWS))
    {
      tracepoint.x = i;
      tracepoint.y = y + deltay;
      tracepoint.elev = get_point (i, y + deltay);
      if (find_zenith_angle(startpoint, tracepoint) < minzenithangle)
      {
        minzenithangle = find_zenith_angle(startpoint, tracepoint);
        minzenithpoint.x = i;
        minzenithpoint.y = y + deltay;
        minzenithpoint.elev = tracepoint.elev;
```

```
      }
    }
  }

  return minzenithpoint;
}

void read_file (void)
{
  unsigned long i;

  rewind (infile);
  for (i=0; i<(unsigned long)ROWS*(unsigned long)COLS; i++)
    fscanf (infile, "%d", fptr+i);
}

void get_UTM_coord (int x, int y, double *UTMN, double *UTME)
{
  *UTMN = N_DOWN_LEFT + ((N_UTM_RANGE / (ROWS-1)) * y);
  *UTME = E_DOWN_LEFT + ((E_UTM_RANGE / (COLS-1)) * x);
}

struct mytime calc_DEM_rise (int doy, int x, int y, double decl,
                             struct point_data *pt)
{
  double UTMN, UTME, convlat, convlong, ha, zeni, azi;
  int minutes, t;
  struct mytime normaltime;
  struct point_data temp;

  get_UTM_coord (x, y, &UTMN, &UTME);
  UTMtoLL (14, UTMN, UTME, UTMZONE, &convlat, &convlong);
  normaltime = calc_rise_set (doy, convlat, convlong, RISESET_ZENITH, 0);
  normaltime.hour = normaltime.hour + TIME_ZONE;
  minutes = (normaltime.hour * 60) + normaltime.minute;
  temp.x = x; temp.y = y; temp.elev = get_point(x, y);

  for (t = minutes;  t<24*60; t++)
  {
    ha = solar_hour_angle(true_solar_time((int) t / 60,(int) t % 60, 0,
      time_offset(equation_of_time(fractional_year(doy)), convlong)));
    zeni = zenith_angle(convlat, decl, ha);
    azi = azimuth_angle (convlat, rtd*zeni, decl);
    *pt = trace_for_sunrise (x, y, azi-M_PI_2);
    if (find_zenith_angle(temp, *pt) >= zeni)
    {
      normaltime.hour = (int) t / 60;
      normaltime.minute = (int) t % 60;
      return normaltime;
    }
  }
  printf ("ERR CALC DEM RISE\n");
  return normaltime;
}
```

```
struct mytime calc_DEM_set (int doy, int x, int y, double decl,
                            struct point_data *pt)
{
  double UTMN, UTME, convlat, convlong, ha, zeni, azi;
  int minutes, t;
  struct mytime normaltime;
  struct point_data temp;

  get_UTM_coord (x, y, &UTMN, &UTME);
  UTMtoLL (14, UTMN, UTME, UTMZONE, &convlat, &convlong);
  normaltime = calc_rise_set (doy, convlat, convlong, RISESET_ZENITH, 1);
  normaltime.hour = normaltime.hour + TIME_ZONE;
  minutes = (normaltime.hour * 60) + normaltime.minute;
  temp.x = x; temp.y = y; temp.elev = get_point(x, y);

  for (t = minutes;  t>0; t--)
  {
    ha = solar_hour_angle(true_solar_time((int) t / 60,(int) t % 60, 0,
      time_offset(equation_of_time(fractional_year(doy)), convlong)));
    zeni = zenith_angle(convlat, decl, ha);
    azi = azimuth_angle (convlat, rtd*zeni, decl);
    *pt = trace_for_sunset (x, y, azi-M_PI_2);
    if (find_zenith_angle(temp, *pt) >= zeni)
    {
      normaltime.hour = (int) t / 60;
      normaltime.minute = (int) t % 60;
      return normaltime;
    }
  }
  printf ("ERR CALC DEM SET\n");
  return normaltime;
}

void main (void)
{
  double decl, UTMN, UTME, convlat, convlong;
  struct point_data minzenpt;
  struct mytime rstime1, rstime2;
  struct mydate monthlist[12] = {{2004, 12, 21}, {2004, 1, 21},{2004, 2, 21},
                      {2004, 3, 21},{2004, 4, 21},{2004, 5, 21},
                      {2004, 6, 21},{2004, 7, 21},{2004, 8, 21},
                      {2004, 9, 21},{2004, 10, 21},{2004, 11, 21}};

  int tempx, tempy, d, day, total;

  if ((fptr = malloc(ROWS*COLS*sizeof(int))) == NULL)
  {
    printf ("ERROR: Can not allocate enough memory. Exiting.\n");
    return;
  }
  outfile = fopen ("results.txt", "w");
  infile = fopen ("wholeDEM.txt", "r");
  read_file();
  fprintf (outfile, "   UTME     UTMN 21DECA 21DECB 21JANA 21JANB 21FEBA
21FEBB 21MARA 21MARB 21APRA 21APRB 21MAYA 21MAYB 21JUNA 21JUNB
```

```
21JULA 21JULB 21AUGA 21AUGB 21SEPA 21SEPB 21OCTA 21OCTB 21NOVA
21NOVB AVRG\n");

  for(tempx=160; tempx<COLS-160; tempx++,printf("%d ", tempx))
  for (tempy=80; tempy<ROWS-80; tempy++)
  {
    get_UTM_coord (tempx, tempy, &UTMN, &UTME);
    fprintf (outfile, "%7d%9d", (int)UTME, (int)UTMN);
    UTMtoLL (14, UTMN, UTME, UTMZONE, &convlat, &convlong);
    total = 0;
    for (d = 0; d < 12; d++)
    {
      day = day_of_year (monthlist[d]);
      decl = declination_angle(fractional_year(day));

      rstime1 = calc_rise_set (day, convlat, convlong,RISESET_ZENITH, 0);
      //rstime1.hour = rstime1.hour + TIME_ZONE;
      rstime2 = calc_rise_set (day, convlat, convlong,RISESET_ZENITH, 1);
      //rstime2.hour = rstime2.hour + TIME_ZONE;
      fprintf (outfile,"%7d",(rstime2.hour-rstime1.hour)*60+(rstime2.minute-
rstime1.minute));

      rstime1 = calc_DEM_rise (day, tempx, tempy, decl, &minzenpt);
      rstime2 = calc_DEM_set (day, tempx, tempy, decl, &minzenpt);
      fprintf (outfile,"%7d",(rstime2.hour-rstime1.hour)*60+(rstime2.minute-
rstime1.minute));
      total += (rstime2.hour-rstime1.hour)*60+(rstime2.minute-rstime1.minute);
     }
    fprintf(outfile, "%5d\n", total/12);
  }

  printf ("Finished. Press Enter.\n");
  tempx = getc(stdin);
  free(fptr);
  fclose(infile);
  fclose(outfile);
}
```

APPENDIX C

SETTLEMENT DATABASE

ID	NAME	UTME	UTMN
1	Doganlar_F29c	494306	4543511
2	Sakarca	588203	4471546
3	Cukurkoy	488499	4552879
4	Guneykisla	590714	4469057
5	Bicikler	487351	4553278
6	Abdullar_F29c2	494240	4553805
7	Gulefler	495032	4553659
8	Akcapinar_F29	495340	4554389
9	Tepe_F29c2	494150	4555100
10	Bayanpinar	585069	4478057
11	Purahmetler	493650	4553350
12	Kavlakli	587293	4469754
13	Bostanli	569388	4464980
14	Sarilar	498882	4553922
15	Yunuslar_F29c	498100	4553950
16	Toklar	497702	4553776
17	Bolukoren_F29	493415	4539491
18	Ortaca	494050	4540950
19	Akbiyik	489950	4541900
20	Hatipoglu	494576	4542682
21	Pelitcik	490522	4540343
22	Kizik	490787	4539191
23	Tasoglu	497700	4539350
24	Yayaoglu	497600	4540050
25	Dokuk	499400	4539050
26	Yakakoy	495650	4539150
27	Terzi_F29c3	495550	4539500
28	Muratoglu	496100	4539550
29	Komesler	496550	4539900
30	Zayim	490750	4541300
31	Ovacik_F29c3	493192	4547347
32	Gümüsler	492227	4547674
33	Sabanlar	493700	4547250
34	Esenler_F29c3	495200	4547100
35	Ahmetler	498970	4550201
36	Colak	499650	4550100
37	Sofular_F29c3	499750	4549650
38	Aydinlar	498550	4549100
39	Bakirci	497950	4548950
40	Alinca	490150	4545800
41	Asagi_Alinca	499776	4544383
42	Ekincik_F29c3	495019	4548725
43	Inceoglu	495900	4548550
44	Kadi	495597	4548297
45	Yayalar	496050	4547950
46	Musatlar	496850	4548750
47	Ganibeyler	491329	4552070
48	Karagol	490528	4551539
49	Karsi	491831	4551587
50	Gumelik	498184	4552600
51	Sutcu	497052	4552282
52	Sindire	496850	4551750
53	Inandik	547741	4473441
54	Bedirler	491427	4543453
55	Sogutcu_Kuzey	490326	4544241
56	Sogutcu_Guney	490650	4544050
57	Demirciler_F29c	491852	4544260
58	Kavaklar	495824	4550625
59	Kargali	495070	4550329
60	Kislakoy	499250	4542750
61	Kislapazari	498800	4542150
62	Cingiller	497950	4542050
63	Koltuk	496850	4542750
64	Ote	497050	4542150
65	Yenioren	494996	4552591
66	Osmankoy	496043	4552596
67	Ilyaslar	494151	4552655
68	Bakircilar	495169	4551929
69	Yiginot	499850	4546650
70	Alkisrak	498400	4547450
71	Eskikoy	497050	4545500

72	Buyuk_Bahceli	584117	4473943
73	Yigitler	494500	4544950
74	Omerler_F29c3	493072	4543514
75	Imanlar_F29c3	491795	4543349
76	Caciklar	595982	4476282
77	Basboyunduruk	488803	4539966
78	Dudas	486860	4539902
79	Musallar_F29c4	487300	4540400
80	Kizilelma	486200	4538950
81	Saraycik_H31b3	579559	4461007
82	Karaomer	591072	4481579
83	Beytarla_Y.	457334	4527590
84	Kapakli_H32a1	587875	4478750
85	Beydini	485885	4546690
86	Boyali	485138	4551844
87	Hatlar	484974	4551115
88	Koseler	484950	4551900
89	Mustafaaga	489127	4552428
90	Kucuksu	488117	4552022
91	Surler	488450	4551077
92	Sazkoy	486676	4548174
93	Guney_F29c4	487731	4547531
94	Suluk	487950	4542700
95	Gocek	489134	4544163
96	Derekoy_F29c4	487597	4543702
97	Catak_F29c4	486712	4543682
98	Yukarikayalar	487603	4542095
99	Asagikayalar	487050	4541800
100	Cay_F29c4	486450	4541500
101	Otegece_F29c4	485900	4541650
102	Govez	485500	4541850
103	Samlar	487088	4550527
104	Saylar	486737	4549564
105	Dogancilar	473675	4540964
106	Karaoren_F29d3	472909	4541218
107	Acemler	471682	4540659
108	Kuzyaka	472100	4539920
109	Ozlu_Y_Kuzey	505473	4480712
110	Babalar	461750	4540700
111	Kartak	460750	4540700
112	Yaylar	462930	4539125
113	Kulatkoy	461329	4542695
114	Asagi_Alagoz	580064	4468269
115	Terzi_F29d4	460884	4543073
116	Catak_Bati	537404	4541005
117	Catak_Dogu	536842	4540748
118	Koclu	524657	4540475
119	Feriz	522195	4542878
120	Ambarozu	500192	4552874
121	Yahya	502242	4553018
122	Yuvacik	500563	4553965
123	Derekoy_F30d3	519961	4542027
124	Ortakoy	519420	4541357
125	Yaylatepe	515457	4545617
126	Karakuzu	515284	4542276
127	Hacilar_F30d3	515696	4543014
128	Yukari_Karakuzu	515850	4541800
129	Dahanlar	515200	4541300
130	Dere_Karakuzu	515112	4541922
131	Cayircik	513060	4542578
132	Evkadi	513115	4543588
133	Hakalmaz	511291	4545101
134	Goynukoren	512268	4540959
135	Hasanlar_F30d3	511976	4541184
136	Camdibi	511780	4540344
137	Dere_Goynukor	512250	4540150
138	Imatlar	512354	4540406
139	Sogucoluk	511203	4539363
140	Harmancik	518445	4543652
141	Belen_Guney	502800	4539850
142	Belen_Kuzey	502600	4540150
143	Samli	502050	4540400
144	Sonya	501721	4542133
145	Kahvecikoy	502203	4542492
146	Dabazali	503600	4542200
147	Ercek_F30d4	500573	4538922
148	Egbeller	500550	4540500
149	Avlagikaya	501420	4545176
150	Emirler	503700	4543700
151	Soganli	502560	4549747
152	Cevre	503773	4551632
153	Asarcik_Kuzey	502250	4551800
154	Asarcik_Guney	501950	4551500
155	Yukarikoy_Soganli	500373	4550321
156	Yaylacilar	503990	4546561
157	Uzumcuk	503619	4548418
158	Istiyehaci	505550	4539950
159	Oluklukoy	505950	4539500

160	Ecik	504602	4541290
161	Istiyetopcu	506197	4539845
162	Ova_Istiyetopc	506186	4541698
163	Kavak	510320	4541266
164	Incekaya_Dogu	507738	4540384
165	Incekaya_Bati	507351	4540349
166	Ekincik_F30d4	508335	4541937
167	Burumcek	507852	4539659
168	Orta_Saraycik	564600	4539162
169	Kumet_Sarayc	564794	4539265
170	Tondur_Sarayc	565283	4539312
171	Comar_Dogu	561644	4542779
172	Comar_Bati	562403	4542849
173	Eksik	556932	4541291
174	Kiymik	557058	4540226
175	Mulayim	559173	4541454
176	Duz	559600	4541650
177	Murathaci	558785	4541560
178	Donayse	558508	4541099
179	Yenice_F31d3	560172	4542248
180	Yuvademirciler	560620	4540053
181	Kissenir	559789	4540222
182	Bolme	446600	4526974
183	Hasanlar_G28b	444136	4535293
184	Salmanlar	445806	4536188
185	Imamlar_G28b	445235	4536655
186	Kozdere	445539	4536882
187	Kayalar	446632	4537224
188	Derekoy_G28b	446733	4537785
189	Adiller	448112	4527637
190	Belen	456379	4534825
191	Eskioglu	456555	4535320
192	Orta_Belen	455833	4534146
193	Dagci	455380	4534093
194	Budaklar	457424	4532444
195	Baldanlar	457839	4532465
196	Buyukyayalar	455767	4531311
197	Haciahmetler	456830	4530511
198	Eleler	456410	4530728
199	Durmuslar	455055	4530555
200	Cotler	454842	4531522
201	Hamzalar	452936	4529272
202	Derekoy_Hamz	453764	4529566
203	Seviller_Guney	453700	4530350
204	Burnuk	454588	4528808
205	Seviller_Kuzey	453475	4530800
206	Kagizlar	457716	4537313
207	Akgozoglu	457549	4536526
208	Dereagil	456890	4537835
209	Haliccik	457184	4536034
210	Yaplan	455910	4537094
211	Akpinar	454302	4536952
212	Kazlarkoy	453702	4537073
213	Kabaarmut	451183	4527822
214	Sofular_G28b2	448601	4537719
215	Karakoy	448004	4538371
216	Oren_Sofular	449651	4537982
217	Kirazlar	450654	4538101
218	Cayli_G28b2	457108	4530155
219	Cokusler	457644	4529191
220	Asagikoy_Cayli	458000	4529386
221	Guvez	456631	4529169
222	Kadirgil	456329	4529407
223	Sevkiler	451487	4531982
224	Oruclar	451518	4531808
225	Turkmenler	451048	4531718
226	Imciler	450728	4530741
227	Demirciler_Sof	449262	4530357
228	Yaziboyu	453953	4532370
229	Seyhler_G28b2	453107	4531856
230	Tasmanlar_G2	453731	4533500
231	Yurecik	452529	4534877
232	Mesecik	453098	4535249
233	Esenler_G28b2	453532	4534855
234	Bekirkoy	453382	4535315
235	Musalar_G28b	452970	4535715
236	Catacik	454655	4535456
237	Eskipazar	460567	4532864
238	Yorgular	460519	4531168
239	Kincilar	460122	4531266
240	Kurban	459428	4532341
241	Istasyon	460607	4534060
242	Arslanlar	462899	4532933
243	Gevrekler	463526	4531549
244	Ahirtas	464341	4531546
245	Dibek	464540	4531943
246	Bayindir_G29a	466646	4525231
247	Boncuklar	468432	4529175

248	Karkin	467800	4529900
249	Gozlu	463096	4529308
250	Tasmanlar_G2	462608	4529804
251	Tefen	462153	4529583
252	Tepekoy_G29a	461950	4529300
253	Durallar	463835	4528887
254	Oren_G29a1	463528	4527945
255	Kadilar	463430	4526664
256	Deresemail_1	468160	4537084
257	Deresemail_2	468174	4537392
258	Deresemail_3	467250	4536750
259	Deresemail_4	466700	4536400
260	Topcali	468421	4532924
261	Y.Topcali	468302	4533661
262	Hasli	458681	4536468
263	Alagoz	458299	4536910
264	Pasakoy_G29a	458065	4537333
265	Imanlar_G29	466420	4528399
266	Kapicilar	459314	4534003
267	Karahasanlar	464655	4538120
268	Yukari_Hasanlar	464680	4537617
269	Asagi_Hasanlar	465521	4537878
270	Yukari_Saray	464297	4538658
271	Asagi_Saray	464826	4538721
272	Ucevler	466404	4538246
273	Cami	461487	4535057
274	Turpcular	460918	4535288
275	Yeni_Kirankoy	461225	4534952
276	Ces	461618	4534362
277	Koycegiz_G29a	462750	4538100
278	Taslikoy	462050	4537950
279	Cavuslar	462250	4538900
280	Ortakoy_G29a	464292	4529960
281	Yenikoy_G29a	463407	4530186
282	Yukarikoy_G29	463681	4529776
283	Sariahmetler	462350	4530500
284	Ovakoy	460100	4536900
285	Dereozu	459456	4537715
286	Kuplu	458857	4538809
287	Ozankoy	459832	4527989
288	Taslik	460323	4525537
289	Beytarla	458135	4528860
290	Otedag	506995	4539361
291	Yazikavak	466133	4533995
292	Asagi_Keceler	465782	4531748
293	Yukari_Keceler	466853	4531509
294	Kirankoy	461573	4535315
295	Baspinar	473088	4537645
296	Ercek_G29a2	475490	4538642
297	Cayir_G29a2	470862	4537939
298	Hocalar	470600	4537800
299	Softalar	470163	4538016
300	Kurukavaklar	469956	4538084
301	Mahmutlar	468650	4530550
302	Yahyalar	469392	4529674
303	Bolukoren_G29	476619	4529159
304	Kabaca	478519	4528126
305	Mutaflar	478100	4529550
306	Karasu	478150	4531050
307	Cumaderesi	478070	4532307
308	Candirlar	473821	4532768
309	Yemisler	471893	4532183
310	Kizilcapinar	471747	4531075
311	Pelitcik_Candirla	471250	4529950
312	Karsi_Candirlar	471849	4530065
313	Doglacik	474100	4528400
314	Saraycik_G29a2	473757	4526440
315	Yunuslar_G29a	474559	4526214
316	Hatipler	474896	4526695
317	Doganlar_G29a	475900	4527150
318	Sadeyaka_Guney	470936	4526633
319	Sadeyaka_Kuze	471200	4526834
320	Seyhler_G29a2	472195	4525373
321	Sobucimen	478765	4535726
322	Sarimehmet	589995	4483621
323	Tamislar	469842	4532133
324	Emiroglu	469779	4534242
325	Asagikoy_Tamis	470475	4533926
326	Yaka	470907	4534635
327	Doruklar	470050	4535350
328	Yesiller	476918	4534500
329	Koseoglu	476008	4534374
330	Yenikoy_Yesiller	477436	4535488
331	Demirciler_Yesi	478132	4537967
332	Dag	471900	4517750
333	Orta_Kuzdere	475150	4518550
334	Asagi_Kuzdere	474979	4518912
335	Yukari_Kuzdere	475500	4518450

336	Goynukcukuru	471442	4520273
337	Bolukoren_Goyn	472479	4519462
338	Yenikoy_Yukari	478350	4522600
339	Yenikoy_Asagi	478800	4522250
340	Yenikoy_Kuruz	478800	4520050
341	Corduk	476850	4522200
342	Hamamli	470450	4524600
343	Kisac_G29a3	472350	4523750
344	Yesiloren	467450	4518200
345	Deresoplan	462100	4522750
346	Dere_Deresoplan	462157	4524597
347	Gokyeri	461400	4524350
348	Orencik_G29a4	460300	4524150
349	Bozkus_G29a4	458900	4524850
350	Kuzoren_G29a4	466550	4522150
351	Akbas	485841	4527525
352	Beydili	487105	4535108
353	Beymelik	483354	4531843
354	Soguksu	481157	4531999
355	Gocuk	482975	4530631
356	Boduroglu	488796	4536643
357	Besiraga	489341	4536692
358	Yayaoglu	488878	4535654
359	Dagdibi	485332	4538643
360	Kuzoren_G29b1	488431	4528346
361	Meydan	485835	4530065
362	Karakoca	487576	4529618
363	Orenli	479597	4525119
364	Ahilar	480818	4526415
365	Tashanlar	483809	4533767
366	Kizilcaoren	483400	4533900
367	Kocekler	485690	4533621
368	Yiprak	484605	4530558
369	Tohumlar	484078	4529026
370	Kisla_G29b1	482950	4529250
371	Kirenozu	481905	4528872
372	Haydarlar	483050	4534950
373	Gokceler	487600	4531250
374	Gomlekciler	482500	4535150
375	Yenikoy_G29b1	479976	4535656
376	Dogancilar_G29	481332	4535459
377	Kapakli_G29b1	479837	4530635
378	Tokmakoglu	480858	4530705
379	Semerciler	479300	4530100
380	Sallar	479300	4534000
381	Yurekoren	489637	4535740
382	Cedime	496255	4525145
383	Catak_G29b2	496418	4537570
384	Karaagac_G29b	495850	4537600
385	Hankoy	468538	4539225
386	Demirci_G29b2	495596	4538032
387	Cayli_G29b2	492094	4529750
388	Yuruk	491350	4530950
389	Beykoy_G29b2	490073	4531010
390	Yusufoglu_G29b	490350	4528878
391	Govem	493377	4529621
392	Dokecek	491120	4537236
393	Sagiroglu	491005	4536591
394	Deveci	489711	4537514
395	Findicak	499020	4533050
396	Yukari_Findicak	499100	4533450
397	Kabak	496148	4529264
398	Incigez	498465	4529773
399	Sofuoglu_G29b	492919	4535899
400	Sarioglu	492400	4536400
401	Kuzgun	498900	4538250
402	Ulukoy	496145	4532604
403	Asagi_Ulukoy	496100	4532400
404	Incebogaz	475898	4532377
405	Karasar	493573	4532690
406	Seyhler_G29b2	496043	4538022
407	Asagi_Kasar_B	493289	4532310
408	Cerkes	490929	4518082
409	Ahirkoy	495027	4513459
410	Aliozu	495961	4520302
411	Bozoglu	493283	4515002
412	Calcioren	496413	4523928
413	Coroglu	495705	4523501
414	Kadiozu	497901	4518372
415	Karamustafa	498932	4515925
416	Gelik	493595	4521480
417	Ovacik_Gelik	494410	4521920
418	Orenkoy	490041	4514669
419	Seyhdogan	491816	4522212
420	Eymir	490765	4522732
421	Yalakozu	498659	4513160
422	Akhasan	483603	4513489
423	Bayindir_G29b	481204	4519260

424	Ilica_G29b4	483400	4519150
425	Bedil	486281	4520921
426	Balkavak	479159	4523712
427	Karaagac_G29	479847	4524184
428	Nahilar	482149	4524023
429	Kurtcimeni	479800	4521500
430	Dikenli_G29b4	482157	4516376
431	Halkoglu	482464	4511387
432	Boyuncak	480485	4512011
433	Kadikoy	484465	4517482
434	Yalnizca	483660	4515681
435	Comlekci	485301	4516882
436	Kizillar	487631	4522333
437	Kinik	489150	4520250
438	Kiremitci	488311	4516951
439	Turbasi	487864	4514457
440	Yortan	486168	4514842
441	Karga_G29b4	484750	4511750
442	Orencik_G29b4	485293	4512412
443	Abdullar_G29b	485950	4511900
444	Agacakoy	482450	4509250
445	Kisac_G29c1	485193	4507401
446	Saraycik_Kuze	480366	4510560
447	Saraycik_Gune	480150	4510750
448	Yakuplar	488951	4509126
449	Yoncali	480975	4506067
450	Yumakli	479399	4508091
451	Yukari_Yumakli	478984	4507615
452	Bozcaarmut_K	484253	4504919
453	Bozcaarmut_G	484200	4505100
454	Dagcukuroren_	486532	4509268
455	Omerler_G29c	486646	4510105
456	Asagi_Dagcuk	487470	4507131
457	Gokce	488155	4506680
458	Elpirek	488206	4507121
459	Hacilar_G29c2	497842	4506110
460	Buguroren	499729	4499561
461	Elden	496233	4500700
462	Dere_Bayindir	498813	4492196
463	Dodurga_G29c	499047	4494701
464	Orta_Bayindir	498764	4490665
465	Tumtac_bayindir	497672	4489225
466	Karga_G29c3	495825	4491348
467	Kayioren	494872	4492608
468	Incecik	492305	4492577
469	Pasanin_ciftligi	592409	4478006
470	Karadibek	585921	4476181
471	Karamursel	588974	4475211
472	Afsar	500368	4529547
473	Erencik	500815	4530114
474	Kiran	502806	4530187
475	Kolavlaga	503495	4530524
476	Cakmak	502750	4536250
477	Dodurga_G30a	501000	4532450
478	Eyupozu	508813	4527587
479	Karacahuyuk	502556	4532943
480	Kizilibrik_G30a	503087	4527548
481	Orta_Kukurt	504500	4529650
482	Demirciler_Kuk	505877	4529907
483	Zevdes	505850	4530950
484	Yazioren_Kuze	509272	4532192
485	Yazioren_Gune	509101	4532436
486	Kiyan	509350	4531050
487	Kisla_G30a2	510559	4530995
488	Ucgazi	507415	4532332
489	Cakirbag	505181	4535658
490	Karaoluk	505079	4537882
491	Sazak_G30a1	507190	4537883
492	Gokcukur	508210	4537883
493	Alic	517722	4535893
494	Akseki	519073	4536397
495	Basovacik	515200	4527700
496	Bayramoren	517100	4532650
497	Beykoy_G30a2	516378	4535022
498	Kopurlu_G30a2	516700	4534075
499	Akguney	513950	4531000
500	Catkese	517850	4526700
501	Dalkoz_Gune	519942	4533096
502	Dalkoz_Kuzey	519796	4533706
503	Dolaslar	514083	4533652
504	Sarikaya_G30	514410	4535044
505	Yilmaz	469234	4542747
506	Kemer_Yurtp	512774	4532564
507	Cayir_G30a2	512168	4532182
508	Madenli	520524	4527108
509	Yusufoglu_G	512750	4533150
510	Doganci	512251	4533103
511	Yukarikoy_G3	512424	4533393

512	Karakisla	513300	4533395
513	Dolap	511127	4532674
514	Yakali_Koyu_O	511479	4528686
515	Yakali_Koyu_K	510688	4528557
516	Yakali_Koyu_D	512200	4529150
517	Asagi_Kasar	493544	4532336
518	Akcaoren_F2	459341	4542526
519	Dagtarla	517006	4519253
520	Dagoren	519606	4512034
521	Yesiloz_G30a	516418	4523952
522	Bozkus_G30a	512056	4520081
523	Budakpinar	512164	4522505
524	Cardak	510879	4517465
525	Cavundur	514418	4518752
526	Sacak	501248	4514658
527	Atkaracalar	506205	4518244
528	Ilker	506858	4517124
529	Demirli	504500	4521000
530	Ulupinar	509861	4516363
531	Susuz	502114	4519732
532	Huyuk_Koyu	505402	4524668
533	Cirdak	527079	4529897
534	Bogazkaya	523750	4537750
535	Karatas_Kuze	521950	4537850
536	Karatas_Gun	521950	4537550
537	Mayislar	521527	4537582
538	Ketenciler	521336	4537984
539	Oymaagac	521150	4535900
540	Sarialan	529944	4535519
541	Pinarcik	527446	4534691
542	Belenli	523200	4534150
543	Uzunoglu	526254	4536387
544	Caylıca	521718	4529435
545	Timarli	580240	4466186
546	Sogutcuk	533603	4526301
547	Aluc_Koyu_Do	542034	4536983
548	Aluc_Koyu_Ba	541247	4536740
549	Asiklar	538108	4530924
550	Eskice	541800	4529200
551	Yenice_G30db	535507	4525076
552	Guney	539740	4530413
553	Ikikavak	535635	4530708
554	Gokceyazi	541632	4535026
555	Mehmetler	540150	4535400
556	Kavakli_G30b2	539442	4526407
557	Kayi	537340	4532123
558	Kirislar	540668	4532240
559	Otegece	540687	4531916
560	Terzi_G30b2	541338	4533307
561	Bahadun	541571	4531223
562	Kizilibrik_G30b	537003	4527081
563	Yesildumlupina	533013	4529996
564	Beloren	541796	4523809
565	Corekciler	538709	4522747
566	Agilozu	533633	4523708
567	Eskiahir	535500	4521000
568	Golluce	534342	4518395
569	Kizilca	532512	4520943
570	Kursunlu	522147	4521052
571	Bereket	525390	4522285
572	Bespinar	523368	4522897
573	Cukurca	526813	4518399
574	Manastir	526116	4517279
575	Hacimuslu_Asa	525538	4524534
576	Hacimuslu_Yu	525046	4524853
577	Hocahasan	529087	4515152
578	Igdir_G30b4	523983	4518757
579	Kapakli_G30b4	523692	4512299
580	Kopurlu_G30b4	524238	4514491
581	Sivricek	531422	4523945
582	Sumucak	529150	4519691
583	Yamukoren	530270	4518067
584	Taskaracalar	523135	4507356
585	Bugay_G30c2	541329	4507159
586	Cukuroren	533844	4501555
587	Yolkaya	538308	4503719
588	Demircevre	538997	4508026
589	Kayiici	539145	4505582
590	Ortayaka	535189	4500017
591	Ciftlikkoy	541911	4493523
592	Eldivan	542307	4486890
593	Cukuroz	537427	4495373
594	Akcali	539463	4496158
595	Saraykoy	540908	4486883
596	Seydikoy	539708	4492243
597	Capar	532613	4483603
598	Caparkayi	529615	4484363
599	Gurpinar	525729	4485264

600	Kamis	528894	4489131
601	Yalak_Cukuroren	501628	4508976
602	Orta	509081	4497604
603	Kalfat	508470	4501961
604	Kanlica	507331	4497733
605	Kisac_G30d1	502434	4499486
606	Salur	505194	4499567
607	Demircioren	518054	4509958
608	Yayla	516323	4508869
609	Dumanli	520202	4504661
610	Sunurlu	516705	4507030
611	Doganlar	516784	4502767
612	Karaagac_G30	514401	4498133
613	Kirsakal	512699	4501052
614	Sakaeli	514161	4503318
615	Sancar	515327	4500267
616	Bulduk	517337	4487998
617	Cerci	517966	4485527
618	Akcaoren_G30	515489	4485874
619	Elmali	510978	4488567
620	Karaoren_G30	520852	4484065
621	Yenice_G30d3	519057	4489896
622	Huyuk_Koy_G3	515350	4493181
623	Eskiyayla	516777	4495080
624	Sakarcaoren	512619	4496652
625	Yaylakent	508193	4493500
626	Inkilap	503329	4490591
627	Yesilyurt_G30d	500635	4484230
628	Ozlu	505249	4485633
629	Bugduz	504494	4495075
630	Gokceoren	504689	4489242
631	Kucukbahceli	583702	4472042
632	Kayilar	507491	4487673
633	Kucukkayi	507215	4489237
634	Yuva	503111	4496647
635	Akcaoren_G31	542894	4534783
636	Alibey	543499	4534453
637	Alibey_Asagi	543950	4533950
638	Karatas	544340	4532516
639	Alpagut	545606	4530091
640	Asagi	549945	4535125
641	Belsogut	550649	4533194
642	Yaylaoren	542463	4527709
643	Yenidemirciler	543158	4527761
644	Basdibek	548471	4526818
645	Danisment	548102	4536197
646	Imamlar_G31a	548650	4536214
647	Gaziler	550837	4527575
648	Caltipinar	549027	4531411
649	Kese	552312	4533453
650	Okcular	544824	4535205
651	Odemis	546810	4533436
652	Omerli	544808	4527440
653	Sagirlar	545916	4525674
654	Seki	546741	4536075
655	Serceler	548690	4537307
656	Kisla_G31a1	548755	4536548
657	Suleymanhacila	542524	4529998
658	Yukari_Bozan_G	549403	4535739
659	Hasanhaci	504211	4493477
660	Ilgaz	552938	4530688
661	Arpayeri	562219	4534762
662	Asagi_Dere	553050	4533950
663	Menser	553370	4533903
664	Kisla_Asagider	553050	4536500
665	Asagi_Meydan	554826	4535425
666	Beykoy_G31a2	561700	4538050
667	Kisla_Beykoy	562472	4538183
668	Ecizoglu	562232	4538036
669	Kuzgece	562207	4537802
670	Bukcuk	555742	4531589
671	Candere	554859	4530645
672	Yuvasaray	562619	4525264
673	Hacihasan	556915	4530125
674	Inkoy	554995	4528323
675	Kalekoy	554974	4534179
676	Kazancı	559212	4538988
677	Kurmalar	560941	4537938
678	Musakoy	557256	4535355
679	Onac	557783	4536416
680	Sarmasık	559298	4525684
681	Satilar	560373	4537378
682	Sazak_G31a2	560267	4533425
683	Sihlar	555842	4536226
684	Yalaycik	559311	4537866
685	Yazikoy	553342	4532362
686	Yerkuyu	560810	4528346
687	Yukaridere	553150	4534250

688	Yukari_Meydan	554737	4535869
689	Yuvademirciler	561200	4538750
690	Derecati	556842	4511945
691	Yukari_Bozan_K	549203	4536093
692	Ilisilik	558616	4521024
693	Kuscayiri	554377	4523577
694	Sezgin	556156	4520645
695	Ahlat	551667	4512399
696	Dikenli_G31a4	544655	4515695
697	Kesecik	546250	4517367
698	Karatepe	546775	4515134
699	Aktas	548308	4523004
700	Ericek	546828	4520098
701	Kiyisin	551080	4520096
702	Kuyupinar	550732	4523316
703	Mesutören	548490	4519766
704	Seyhyunus	544315	4521297
705	Boyacioglu	587305	4478011
706	Saraycik_G30b	564416	4539032
707	Asagi_Oz	574970	4518979
708	Ayseki	575900	4515350
709	Pirkayip	577127	4516889
710	Bademcay	582690	4513598
711	Cakirlar	583158	4514448
712	Davutlar	582442	4515714
713	Saraycik_G31b	583154	4516295
714	Kivcak	574390	4513615
715	Sarikaya_G31b	580305	4518279
716	Gokceyuz	579578	4516948
717	Yaka_Koy	579892	4515687
718	Asagikaya	578844	4514609
719	Yukariyaka	580391	4515770
720	Yesilyurt_G31b	577428	4514120
721	Yaprakli	565769	4512238
722	Akyazi	569892	4511439
723	Igdir_G31b4	568790	4514013
724	Kavak_Koyu	570077	4515572
725	Yukarioz	570694	4518333
726	Hasakca	564928	4501842
727	Bugay_G31c1	564177	4508154
728	Buluca	568085	4509374
729	Doganbey	571670	4507165
730	Karacaozu	565343	4509106
731	Cevrecik	572187	4501167
732	Sazcigaz	567961	4506220
733	Yenice_G31c1	571679	4504602
734	Yuklu_Bati	567179	4503781
735	Yuklu_Dogu	567872	4504052
736	Ayvakoy	583181	4509369
737	Yukariayva	582532	4510621
738	Cercicami	584293	4511191
739	Ikizoren	574594	4504691
740	Goynukeren_Y	514109	4538303
741	Yamacbasi	580012	4507085
742	Yabani	581492	4506512
743	Sogutlu	583489	4505292
744	Buyuk_Akseki	580071	4500323
745	Kayacik	581182	4503609
746	Saricay	579837	4502755
747	Kaymaz	576707	4508681
748	Kirliakca	577675	4498291
749	Subasi	578156	4505688
750	Kullar_Guney	579257	4510197
751	Sofuoglu_G31c	580455	4504653
752	Tatlipinar	573994	4508334
753	Topuzsaray	575552	4499318
754	Zekeriyakoy	576998	4502188
755	Kuzukoy	580497	4485855
756	Altinli	581708	4488470
757	Alacat	578279	4491522
758	Haydar	579962	4491118
759	Balibagi	566045	4490459
760	Bayindir_G31c	568940	4497042
761	Cayirpinar	567328	4493177
762	Civikoy	564563	4493873
763	Kucuklu	568826	4493461
764	Ovacik_G31c4	572137	4489100
765	Kaput	573129	4492787
766	Akcavakif	548440	4504939
767	Tepekoy_G31d	548758	4503265
768	Gumusduven	544916	4504023
769	Asagi_Cavus	552070	4504409
770	Ayan	550493	4502656
771	Ikicam	547309	4509671
772	Karatekin	543250	4501971
773	Korgun	543475	4509743
774	Alanpinar	551348	4508749
775	Icyenice	549700	4500700

776	Kembaglari	551375	4499677
777	Basegmez	554412	4510701
778	Ballibidik	561871	4505042
779	Degim	559547	4506219
780	Dutagac	557399	4505618
781	Inac	558804	4498205
782	Pasakoy_G31d	556438	4508616
783	Yakadere	560463	4508317
784	Yukaricavus	553326	4504896
785	Esentepe	555379	4492795
786	Dedekoy_G31d	561814	4494056
787	Dogantepe	554010	4491112
788	Süleymanlı_G3	553158	4486472
789	Tuzlu	557107	4497371
790	Cankiri	551145	4495623
791	Oglakli	546847	4487140
792	Asagi_Yanlar	547939	4489945
793	Golezkayi	545950	4485200
794	Hidirlik	548830	4494307
795	Saritarla	543250	4495064
796	Süleymanli	552421	4485521
797	Saritepe	544808	4491849
798	Cicek	584900	4513050
799	Mansurlu	585940	4513406
800	Musellim	585714	4512195
801	Kilicli	585350	4512500
802	Kayapa	584651	4512167
803	Huseyinfaki	585255	4511743
804	Kerimler	585911	4512037
805	Yesilyayla	587008	4515050
806	Belibedir_Kislac	585445	4511248
807	Belibedir_Cerikl	584700	4510950
808	Kiyi	589809	4499263
809	Hacihasanoglu	590100	4499200
810	Kulla	590336	4499020
811	Imamusagi	590074	4498367
812	Igdecik	590570	4498344
813	Coca	590402	4497846
814	Hacilar_H31b3	574434	4466241
815	Gurmec	585408	4501497
816	Asagikayaharm	587820	4501813
817	Ozlu_Y_Guney	505888	4480014
818	Agzibuyuk	586283	4488742
819	Mollamehmet	585565	4488447
820	Kazbekir	588259	4489283
821	Haciomer	587542	4489943
822	Danabasi	588480	4486346
823	Yeniyapan_G32	587171	4485451
824	Bascoban	590822	4487707
825	Kizara_Y	510750	4537578
826	Karadayi	567033	4467242
827	Kizilirmak	583590	4466986
828	Besdut_Guney	590172	4496480
829	Besdut_Kuzey	590400	4497464
830	Cagabey	587759	4494083
831	Unur_Koyu_Kuz	584967	4493630
832	Unur_Koyu_Gu	584944	4492537
833	Tepealagoz	582310	4469719
834	Buyuk_Yakali	517806	4481699
835	Kosrelik	512339	4477424
836	Kutlusar	519612	4472599
837	Kurtsivrisi	518562	4469652
838	Kucuk_Yakali	517597	4480430
839	Yesiloz_H30a2	517900	4477000
840	Sarisu	515750	4472700
841	Tepekoy_H30a	516750	4473150
842	Mese_Y_H30a3	513455	4467797
843	Dalyasan	513200	4469300
844	Demirci_H30a2	518590	4464914
845	Meseli	517634	4468013
846	Oyumigde	519259	4463796
847	Ozbek	520450	4468750
848	Sabanozu	524011	4481555
849	Bulgurcu	522095	4474068
850	Goldagi	522079	4472556
851	Gumerdigin	521677	4477158
852	Demirhasan	526298	4474658
853	Gundogmus	524866	4470647
854	Karakocas	531022	4477772
855	Odek	525105	4472370
856	Hisarcik	538733	4472524
857	Hisarcikkayi	540801	4474172
858	Bakirli	532062	4479847
859	Martkoy_Kuzey	533675	4475539
860	Martkoy_Guney	533871	4475112
861	Karamusa	521647	4466041
862	Karahaci	524071	4467532
863	Akoren	550296	4474927

864	Buyuk_Hacibey	543341	4475920
865	Elmaci	546835	4480650
866	Golez	546583	4483116
867	Alica	571099	4467234
868	Terme	550867	4470796
869	Kucuk_Hacibey	544111	4478025
870	Yukari_Pelitozu	551985	4480496
871	Akbulut	544365	4481764
872	Asagi_Pelitozu	555318	4479450
873	Germece	557444	4473427
874	Konak	554208	4471409
875	Bozkir	572188	4477551
876	Dedekoy_H31b	566116	4478528
877	Ciftlik	564944	4479319

878	Asagi_Ovacik	574226	4478497
879	Yukari_Alagoz	577032	4471457
880	Yeniyapan_H3	578905	4477612
881	Yuvalar	485381	4539486
882	Acioz	469172	4542114
883	Yukari_Caykoy	468609	4541244
884	Buyuktarla	469704	4542593
885	Yurtpinar	513122	4532922
886	Kullar_Kuzey	579603	4510466
887	Icmederesi	591052	4498846
888	Yaylakent_Y	500080	4482983
889	Kayi_Y	509759	4481769
890	Osmanbey	586346	4478060
891	Adiller_Y	445793	4527602